2013•2014

FACULTEIT INDUSTRIËLE INGENIEURSWETENSCHAPPEN

master in de industriële wetenschappen: nucleaire technologie

Masterproef

Improving the radionuclide Inventory Determination of the Irradiated Graphite from BR1 in Mol

Promotor :
Prof. dr. Wouter SCHROEYERS

Promotor :
Prof. ir. PIERRE VAN ISEGHEM
dr. EDOUARD MALAMBU MBALA

Stefan Nijst

Proefschrift ingediend tot het behalen van de graad van master in de industriële wetenschappen: nucleaire technologie

KU LEUVEN | universiteit hasselt

Abstract

The Belgian Reactor 1 (BR1) operational since 1956 at SCK·CEN in Mol, is the oldest research reactor in Belgium. It is a graphite-moderated and air-cooled reactor fuelled with natural metallic uranium. The active core consists of a 6.66 x 6.84 x 6.84 m^3 graphite matrix, built by stacking squared-base prismatic graphite blocks (~14500), yielding a total mass of 492 tons.

The BR1 is supposed to continue its operation for several decades; however it is necessary to already make studies about the activity level of the graphite which is related to the disposal scenario. The objective of this study was to determine the radionuclide inventory to be expected at the dismantling due date in the irradiated graphite. Those radionuclides have formed by neutron activation process following nuclear reactions between the neutrons and stable nuclides present in the graphite as main component or as impurities. The radionuclide build-up rate is a function of the initial atom content (which is different for graphite A and B quality), of the neutron flux, of the activation reaction cross sections, of the position inside the reactor and on irradiation conditions and history.

In this work a numerical simulation of the irradiation of the BR1 full core including the fuel elements and many graphite samples selected in various neutron field positions was carried out. The Monte Carlo burn-up code ALEPH was used for the calculation. In 2011, SCK·CEN performed a few gamma spectrometry measurements on the irradiated graphite A test sample collected in channel C2.3 of the BR1 core lattice. These results will be used to validate the computer model. Together with the current acceptance criteria for surface disposal, published by NIRAS/ONDRAF we will discuss which volumes were suited for surface either geological disposal.

Abstract – Dutch

De BR1 (Belgische Reactor 1) is operationeel sinds 1956 op de site van het SCK·CEN te Mol en is de oudste onderzoeksreactor in België. Het is een grafiet-gemodereerde, luchtgekoelde reactor, met natuurlijk uranium als brandstof. Het hart van de reactor bestaat uit een 6,66 x 6,84 x 6,84 m^3 grafiet matrix, gebouwd door het stapelen van prismatische blokken (~ 14500), met een totale massa van ongeveer 492 ton.
De BR1 is verwacht nog meerdere decennia operationeel te blijven. Toch is het reeds nu al noodzakelijk om studies uit te voeren over het activiteitsniveau van het grafiet, hetgeen gerelateerd is aan de bergingskost. Het doel van deze studie was om de radionuclide samenstelling van het bestraalde grafiet te bepalen op het tijdstip wanneer de reactor zal ontmanteld worden. Deze radionucliden werden geproduceerd door neutronenactivatie als gevolg van nucleaire reacties tussen de neutronen en stabiele nucliden in het grafiet, als natuurlijk voorkomend nuclide of als onzuiverheden. De radionuclide productiesnelheid is een functie van de oorspronkelijke onzuiverheidsconcentraties (verschillend voor grafiet kwaliteit A en B), het BR1 werkingsregime, de neutronenflux en de activatie werkzame doorsnede. Voor deze studie werd de numerieke simulatie software ALEPH, een Monte Carlo activatiecode gebruikt. De simulatie van de gehele reactorkern, inclusief de brandstof en 44 grafietstalen op uiteenlopende locaties gepositioneerd werd voltooid. De simulatieresultaten konden voor enkele radionucliden vergeleken worden met gammaspectrometrie metingen van 2011. De evolutie van cruciale radionucliden op diverse posities werd geanalyseerd. Tot slot werd met de huidige acceptatiecriteria een voorlopige uitspraak gedaan over de bergingsoptie van de grafietstalen.

Acknowledgement

First of all I would like to thank Mr. Pierre Van Iseghem for presenting this topic and give me the permission to start the thesis at SCK·CEN. Also his advice and guidance were of big importance.

I would like to thank Mr. Edouard Malambu for his help, advice and training during the work, especially the computer simulations, which I needed to discover. He is a good teacher and scientist at the same time and was always available for support.

My thanks go to Mr. Wouter Schroeyers, my University Promoter for his advice and guidance for formulating and progression in writing the thesis.

I would like to thank all the persons at SCK·CEN who were related to this work and always shared their knowledge with pleasure.

Finally thanks to my parents for allowing me to start the thesis in Mol and their interest during the year.

List of Abbreviations

ALEPH	: A Monte Caro Burn-up Code (developed by SCK·CEN)
BR1	: Belgian Reactor 1
FANC	: Federal Agentschap voor Nucleaire Controle / Federal Agency for Nuclear Control
IAEA	: International Atomic Energy Agency
ICP-AES	: Inductively Coupled Plasma Atomic Emission Spectroscopy
LANL	: Los Alamos National Laboratory
MAGNOX	: UK type of graphite-moderated air-cooled nuclear reactor
MCNP	: Monte Carlo N-Particle transport code (developed by LANL)
ONDRAF/NIRAS	: The Belgian National Agency for Radioactive Waste and enriched Fissile Material
RBMK	: Russian type of graphite-moderated water-cooled nuclear reactor
SCK·CEN	: Studiecentrum voor Kernenergie·Centre d'étude de l'énergie nucléaire

List of figures

List of tables

1 Introduction & background

1.1 Radioactive waste

The production of radioactive waste is the consequence of the beneficial applications of radioactivity. The most significant and well known application of radioactivity in is the production of electricity in nuclear power plants. Radioactive waste is any material which contains radionuclides at concentrations which are above the acceptable values without regulatory control. It means that these materials have higher radiation levels than the clearance levels defined by the government. Because radioactive waste emits high energetic radiation consisting out of subatomic particles which are harmful for the people and the environment, the waste needs a lot of attention. First of all, when dismantling a nuclear installation, the equivalent dose absorbed by the workers need to be as low as possible. Later on, when the waste is conditioned, a suited disposal location need to be selected.
There is a large difference in costs between surface disposal and geological disposal: geological disposal is about 10 times more expensive than surface disposal, which makes it really important to make a good characterization and classification of the waste. There will always be the intention the reduce the volume of high level waste to minimize the costs.
The Belgian classification of radioactive waste is determined by NIRAS/ONDRAF, the national institute for radioactive waste and fission material. In this classification, 3 waste categories are present: category A, B and C. The distinction between those categories is based on the radionuclide inventory and their corresponding activity level. The final repository for the waste is based on its category. Category A, due to is shorter lived radionuclides, it suited for surface disposal while in contrast category B and C are considered for geological disposal. Currently, none of either repositories are operational in Belgium. All the radioactive waste is still temporary stored on the domain of Belgoprocess in Dessel.

1.2 Graphite moderated reactors

Graphite moderated nuclear reactors have been used worldwide for electricity production Most of these reactors are located in the United Kingdom. In the UK, 17 reactors of the type MAGNOX and AGR were built. MAGNOX (Magnesium non-oxidising) refers to the cladding of the fuel rods. The Advanced Gas-cooled Reactor (AGR) is the second generation gas-cooled reactors developed and operating in the UK. This type of reactor still uses graphite as moderator but uses lightly enriched uranium oxide pellets in stainless steel tubes in contradiction to the MAGNOX reactors. Both MAGNOX and AGR are CO_2 cooled graphite moderated reactors and were built during the late 1950's until the mid 1970's. Most of them are currently shut down, only a few are in operation.[1]

Another well-known type reactor which uses graphite is the RBMK. The RBMK reactor is a type of nuclear power reactor designed in the Soviet Union. RBMK is the Russian abbreviation for higher-power channel reactor and is in fact a combination of a pressurized water reactor and a gas cooled reactor. The concept of a graphite moderated reactor cooled by (light) water is unique in the world. For instance, the reactor in Chernobyl was also from the RBMK design. The total number of RBMK reactors is 15. Country based, the division is like the following: 11 in Russia, 3 in Ukraine and 2 in Lithuania. Originally 4 reactors were built in Chernobyl, Ukraine, but reactor 4 was destroyed in April 1986 during an explosion. All the reactors in Ukraine and Lithuania are shut down. In Russia, 9 of them are still operating.[2]

The reactor considered for this work is the BR1, located at the domain of SCK·CEN in Mol, Belgium. The BR1 is a research reactor and operational since 1956 with o nominal power of $4MW_{th}$. The reactor contains about 492 tons of graphite blocks.

Worldwide, about 250 000 tons [3] of nuclear grade graphite is present. Therefor it is a major concern and it is suggested to make studies about the activated graphite of nuclear reactors. At the moment international research institutes have years of research and experience with the CARBOWASTE project. The project deals with the large amounts of irradiated graphite and tries to investigate the best option to condition and treat the waste.

1.3 BR1 Graphite waste

At first sight, all the produced waste is related to the spent nuclear fuel rods. However in reality, more radioactive material is produced besides the nuclear fuel. Construction materials like concrete and metal as well as graphite, present in the core as neutron moderator has transformed into radioactive waste. The BR1 consists out of about 492 tons[4] of irradiated graphite, which corresponds to roughly 300 m^3 of graphite waste and the BR1 is therefore a major producer of waste.

The activation process is responsible for converting virgin graphite into radioactive graphite. During the reactor's operation, neutrons collide with stable elements, mainly present as impurities in the graphite blocks. Nuclides are converted into radionuclides. The major nuclear reactions are (n,γ), (n,p) and (n,α). These impurities are always present due to the manufacturing process. The concentrations of the elements besides carbon can differs from element to element.

Currently, these radioactive blocks are not harmful due to the thick concrete shield surrounding the reactor core. When the BR1 reaches its end of life, it will be dismantled, meaning that all graphite blocks will be removed and disposed as radioactive waste. At the moment, the radioactivity level and radionuclide composition of the graphite at various positions is unknown.

1.4 Previous studies

1.4.1 IGNALIA nuclear power plant RBMK-1500 reactor

In recent years, several papers have been published about the modelling of irradiated nuclear graded graphite with the use of Monte Carlo computer codes. Three papers were consulted from 2005[5], 2009[6] and 2011[7]. They handle about the modelling of impurity activation of irradiated graphite from the RBMK reactor in the Ignalia Nuclear Power Plant. It concerns the RBMK-1500 reactor Unit 1 of the Ignalia Nuclear Power Plant in Lithuania. This unit operated from 1984 until 2004. In the first and second study MCNP is used in combination with CINDER, the 2nd study uses MCNP with ORIGIN-S which is quite similar to our study. However, the RBMK reactors in Lithuania are not research reactors as the BR1, but are used for electricity production. This also translates to the size of the reactors which contain about 3600 tons of graphite, compared to the almost 500 tons of the BR1. The nominal thermal power of the RBMK-1500 is 4250 MW[6] compared to the 4 MW of the BR1. Three orders of magnitude more power will translate to much higher spatial neutron fluxes. For that reason, combined with the almost continuous operation, higher activation will occur in the graphite of these commercial nuclear power reactors and the results of this study concerning specific activity cannot be related to the BR1 because both reactors have been used for different purposes.

In the 2005 study, the activity was modelled at different axial positions in the moderator and reflector of the reactor. The evolution of the specific activity in the moderator, fuel channel sleeves and 3 parts of the reflector, each with a specific neutron flux was calculated in the 2005 study.

The study yields interesting results, however, important results are missing. No 3D zones in the moderator at different axial and radial distances were considered. No final classification of the waste was done, however it was shown that many radionuclides exceeded their clearance levels. In the study it was also mentioned that the specific activity of trans uranium elements in the moderator was significant close to the recommendations limits, set by the IAEA for the acceptance of low and intermediate level waste packages.

The activity values described in these studies are not useful for comparison with the BR1 for several reasons. First of all, the thermal power of the BR1 is much lower, as explained earlier. The geometry of both reactors is different. Also it is not sure if the same graphite quality is used, which has a big impact on the impurity concentrations.

1.4.2 BR1 graphite studies

In 2000, N. Messaoudi[8] carried out the first every study to characterize the radiological compositions of the structural materials of the BR1. The study includes graphite type A and B as well as the concrete shielding. The final results of the study of N. Messaoudi differs considerable to our study because at that time less advanced computer codes and less precise cross section libraries were available. The current computer geometry of the BR1 is much more detailed. A detailed 3D mapping is available for the current study and so no geometrical simplifications like the ones made in 2000, needed to be sued. However, our study will use the same value of 10 ppm (parts per million) for the nitrogen impurity.

Later on, in 2010[9] E. Bravo completed his master thesis "Characterization of irradiated BR1 graphite". These results were more advanced. The measured neutron flux in a cross sectional plane of the BR1 was used from the study in 2010, which was the same as the study performed by N. Messaoudi. The depletion computer code ORIGEN 2.2 was used.

Li and N will produce tritium and C-14 when activated by neutrons (DGNAA technique). These radionuclides are beta-emitters. Because the beta spectrum is a continuous spectrum it is very difficult to determine the individual nuclides from the complex composed spectrum. Another methods is the PGNAA (prompt gamma ray neutron activation analysis), which is measuring the emitted gamma rays immediately during the irradiation by neutrons. In 2010 this technique was not available at SCK·CEN en currently no new measurements have been performed.

The 2010 study uses simulations for several parameters. The first simulations gave an idea of the evolution of activity in time. This was done for ^{3}H, ^{14}C, ^{36}Cl and ^{60}Co both for graphite A and B quality. For ^{14}C, additional calculations were performed to show the difference with and without the 0.05 ppm Li and 10 ppm N. The result for ^{14}C in graphite A is shown in figure 1.1. Different radial distances were used to see the effect of the location dependant neutron flux on the activation of the radionuclides. For graphite A, distances ranged from 0.5 to 236 cm and for graphite B from 272 cm tot 342 cm.

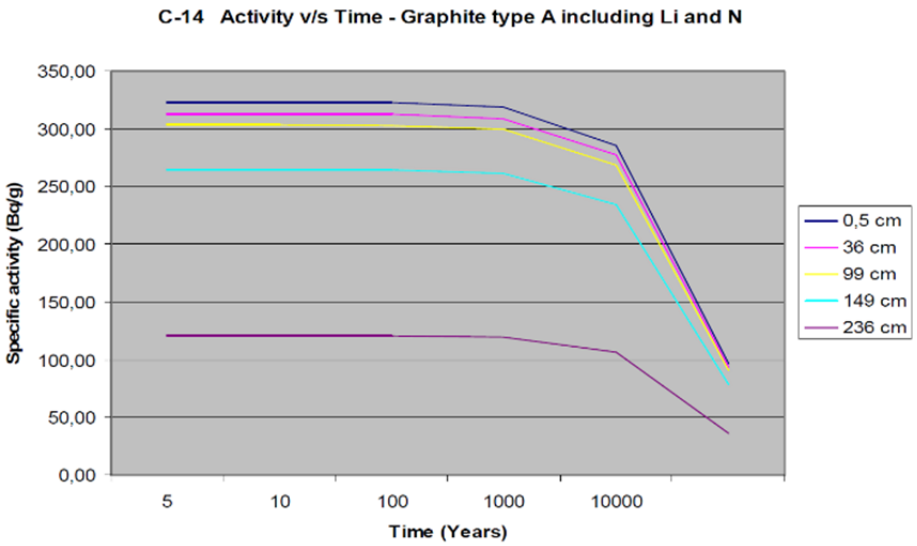

Figure 1.1: Carbon-14 specific activity as a function of time in graphite A.[9]

With the intension to investigate the effect of impurity concentration on the final activity, 14 scenarios were developed. 7 scenarios for graphite A en 7 for graphite B. The difference between the scenario's was the change in concentration of the most important precursors. In that way, the impact of Li, N, Co, Cl was investigated. The activity value for graphite A was calculated at 0.5 cm and at 272 cm for graphite B. In this case the highest possible activity values are reached. For now, there will be focused on Scenario 1,2, 8 and 9. Scenarios 1 and 2 are for graphite A, without and with 0.05 ppm Li and 10 ppm N. The same logic applies for scenarios 8 and 9 that handle graphite B. Scenario 1 and 8 represent the basic activity for each graphite type. This was done because Li and N have never been measured, but the used values were based on literature values[8]. The next graph shows the result for these 4 scenarios at shutdown of the reactor.

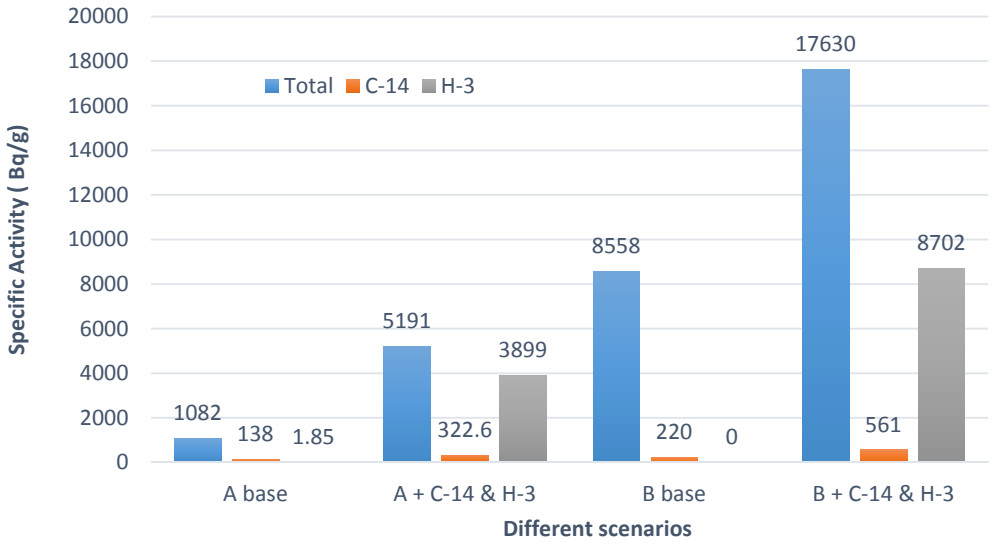

Figure 1.2: Visual representation of result from scenario 1,2,8 and 9. (based on [9])

Figure 1.2 shows a big difference in base concentration between A and B. The reason is that graphite B has much higher activity from ^{152}Eu and ^{63}Ni. When lithium and nitrogen were added, the total concentration increased strongly. The major contribution of this increase is from ^{3}H. ^{3}H has as $T_{1/2}$ of 12.3 years compared to the 5430 years of ^{14}C.

One conclusion that already can be made it the fact that the total specific activity of graphite B is higher than graphite A, 17630 Bq/g compared to 5191 Bq/g. The neutron flux values are higher at the center of the reactor core, where graphite A is located, but graphite B contains higher concentrations of impurities.

To have a first idea of the impact of these result on a final disposal option, the detailed results from scenario 1,2,8 and 9 were used to calculate the X and Y criteria, earlier explained in section 1.4.7.

Graphite type	Scenario	X criterion	Y criterion	Disposal Option
A	1	0,066	7,02	Surface disposal possible
	2	0,066	7,15	
B	8	0,343	37,2	
	9	0,343	37,4	

Table 1.1: Disposal option for several scenario's from BR1 2010 study.

In all the four cases listed in table 1.3, the graphite is ready for a possible surface disposal. This implies that is has a higher than average activity for some of the 20 critical radionuclides

for normal surface disposal. For the X criterion, Niobium 94 was dominant, while Chlorine 36 was dominant for the Y – criterion.

The final conclusion regarding the production of ^{36}Cl. It showed that sulphur and potassium has less impact on the activity of ^{36}Cl compared to the Cl concentration. It is concluded that $^{35}Cl(n,\gamma)^{36}Cl$ is the leading reaction.

In the work of E. Bravo, less information and computer codes were available compared to now, 4 years later. One of the biggest improvements in the current study will be the usage of the Monte Carlo MCNP software. First there is the BR1 3D geometry which was previously reconstructed by E. Malambu based on drawings and the scale model of BR1. Secondly the ability to calculate the neutron flux and spectrum values with high accuracy with MCNP. The previous study did not included any reactor geometry, it only used the flux values, measured at certain points in the axial direction of the graphite, through the center of the core. The concentration of some additional impurities is known by a document form the manufacturer of the graphite. Finally, gamma spectrometry results for certain radionuclides from 2011 are available in order to validate the computer calculation.

1.5 Objectives

The objective of this work is to make the best possible estimation of the radionuclides produced in the irradiated graphite of the BR1 since the start of its operation in 1957. This will be accomplished with the state of the art Monte Carlo Burn-up code ALEPH [10].
This evolution calculation will be performed at different positions in the graphite pile.

The final goal is to categorize the graphite sub volumes for surface or geological disposal based on the current radiological waste acceptance criteria for surface disposal.

Physical measurements will not be carried out during this work, these measurements have been done in the past. Measurements on non-irradiated graphite will be used to determine the material composition of the virgin graphite while measurements of irradiated graphite will be used to validate the computer simulation.

2 Radioactive waste

2.1 Activation process

2.1.1 Nuclear reactions

2.1.1.1 Carbon-14

Carbon-14 is produced by several reactions inside the BR1 graphite.

- ${}^{14}_{7}\mathrm{N}\ (n, \mathrm{p})\ \mathbf{{}^{14}_{6}C}$
- ${}^{13}_{6}\mathrm{C}\ (n, \gamma)\ \mathbf{{}^{14}_{6}C}$
- ${}^{17}_{8}\mathrm{O}\ (n, \alpha)\ \mathbf{{}^{14}_{6}C}$ or in a two-stage process ${}^{16}_{8}\mathrm{O}\ (n, \gamma)\ {}^{17}_{8}\mathrm{O}\ (n, \alpha)\ \mathbf{{}^{14}_{6}C}$

Some reactions are more likely to happen than others. More ^{14}C production originates from ^{14}N than ^{13}C or any other nuclide. Therefore can a very low concentration of ^{14}N result in more ^{14}C production with the same amount of ^{13}C. Only ^{14}N is an impurity, because ^{13}C and ^{17}O are natural occurring isotopes. ^{14}C can form $^{14}CO_2$ and $^{14}CH_4$ and get in the biosphere by gas or groundwater from its disposal location.

2.1.1.2 Chlorine-36

The special characteristic of ^{36}Cl is its halftime of 3.01 x 10^5 years. This implicates that ^{36}Cl is a crucial radionuclide produced in the graphite of the BR1 which will remain radioactive for a very long time. It can be produced in 2 ways, with ^{35}Cl or ^{39}K. ^{35}Cl is the dominant reaction:

- ${}^{35}_{17}\mathrm{Cl}\ (n, \gamma)\ \mathbf{{}^{36}_{17}Cl}$
- ${}^{34}_{16}\mathrm{S}\ (n, \gamma) {}^{35}_{16}\mathrm{S} \rightarrow \beta^- \rightarrow {}^{35}_{17}\mathrm{Cl} (n, \gamma) \mathbf{{}^{36}_{17}Cl}$
- ${}^{39}_{19}\mathrm{K}\ (n, \alpha)\ \mathbf{{}^{36}_{17}Cl}$

2.1.1.3 Tritium

Tritium, an isotope of hydrogen with 2 neutrons is created by the (n,α) reaction of ${}^{6}_{3}\mathrm{Li}$.
Only 6.5% of the natural occurring lithium is ${}^{6}\mathrm{Li}$ which can transmute to ${}^{3}\mathrm{H}$.
Tritium is expected to be present in very high concentration partly due to its short half time of 12.3 years.

- ${}^{6}_{3}\mathrm{Li}\ (n, \alpha)\ \mathbf{{}^{3}_{1}H}$

2.1.1.4 Cobalt-60

${}^{60}_{27}\mathrm{Co}$ is generated from ${}^{58}_{26}\mathrm{Fe}$ which is an isotope of iron and is present in the virgin graphite. However its abundance is 0.29 % , so only a very small fraction of the available iron atoms will be responsible for the formation of ${}^{60}\mathrm{Co}$. Next, the 3 steps of the formation are given:

1) ${}^{58}_{26}\mathrm{Fe}\ (n, \gamma)\ {}^{59}_{26}\mathrm{Fe}$
2) ${}^{59}_{26}\mathrm{Fe}\ (\beta^{-})\ {}^{59}_{27}\mathrm{Co}$
3) ${}^{59}_{27}\mathrm{Co}\ (n, \gamma)\ \mathbf{{}^{60}_{27}Co}$

${}^{59}\mathrm{Co}$ is also present in the virgin graphite as an impurity.

2.1.1.5 Europium

^{152}Eu, ^{154}Eu and ^{155}Eu are radioisotopes of europium

Direct reactions from the stable europium isotopes to the radioactive ones:

- $^{151}_{63}\text{Eu}\ (n,\gamma)\ \mathbf{^{152}_{63}Eu}$
- $^{153}_{63}\text{Eu}\ (n,\gamma)\ \mathbf{^{154}_{63}Eu}$

Indirect reactions of Samarium to produce additional $^{151}_{63}$Eu, $^{153}_{63}$Eu and $^{155}_{63}$Eu.

- $^{150}_{62}\text{Sm}\ (n,\gamma)\ ^{151}_{62}\text{Sm}$, $^{151}_{62}\text{Sm}\ (\beta^-)\ ^{151}_{63}\text{Eu}$
- $^{152}_{62}\text{Sm}\ (n,\gamma)\ ^{153}_{62}\text{Sm}$, $^{153}_{62}\text{Sm}\ (\beta^-)\ ^{153}_{63}\text{Eu}$
- $^{154}_{62}\text{Sm}\ (n,\gamma)\ ^{155}_{62}\text{Sm}$, $^{155}_{62}\text{Sm}\ (\beta^-)\ \mathbf{^{155}_{63}Eu}$

Europium has a high activity but a low $T_{1/2}$ so it's concentration will decrease rapidly.

2.1.2 Basic concepts of activation

The reaction rate (R) is an important concept in the activation process. It shows which parameters influence the transformation of stable elements into radioactive elements due to nuclear interactions. The concept of reaction rate is shown in equation 2.1:

$$R = N \int_0^\infty \sigma(E)\varphi(E)dE \tag{2.1}$$

Where N represents the atom density of the atoms that will be activated, σ(E) the energy dependant reaction cross section and φ(E) the neutron flux spectrum. In order to calculate the true reaction rate, it is essential to integrate over the energy distribution.
The energy of the neutrons is related to the neutron velocity . Therefore, the neutron flux can be written as:

$$\varphi(v) = n(v)v \tag{2.2}$$

Where n(v) is number of neutrons with velocity v per unit of volume.

Once a radionuclide is produced, it will probably undergo natural radioactive decay and its quantity will be reduced over time. Simple radioactive decay is described by a decreasing exponential function given by
equation 2.3.

$$N = N_0 \, . \, e^{-\lambda t} \tag{2.3}$$

Where λ is the decay constant, the probability that a nucleus will decay per unit of time. N is the number of nuclei at time t. The product of the decay constant and the number of nuclei is A, called the activity. The unit is Bq/s and equals the number of desintegrations or radioactive decay's per second. The half-life or $T_{1/2}$ is the time needed to reduce the amount of the initial radionuclide by 50%. This half-life can vary many orders of magnitude from fractions of a second to billion of years. **Error! Reference source not found.**2.1 illustrates the decay of ^{14}C with a $T_{1/2}$ of 5730 years.

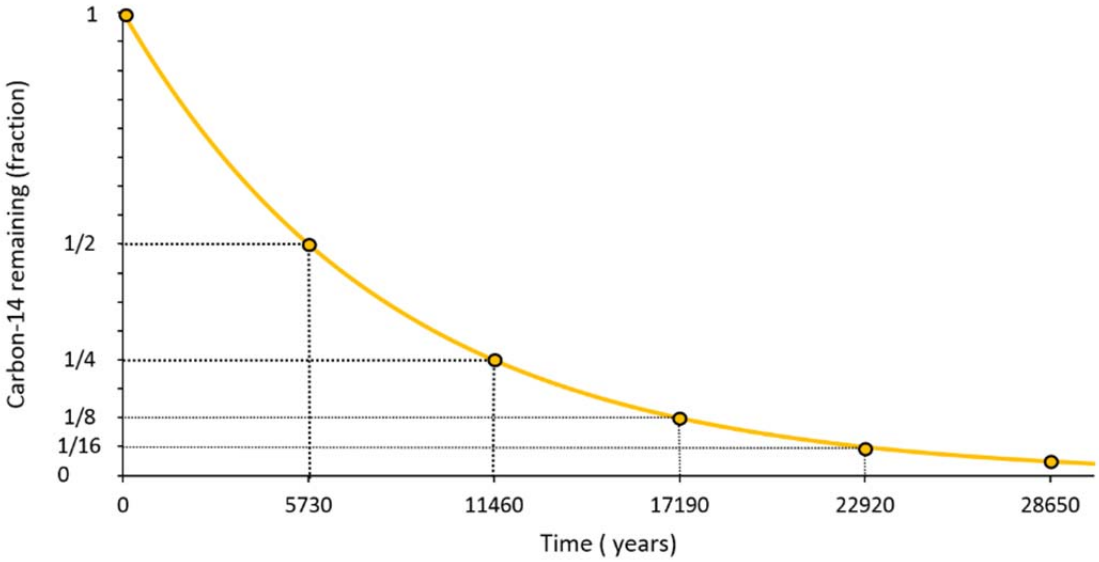

Figure 2.1:Radioactive decay of Carbon-14 as function of time.

As shown in the previous section, the linear transformation between a precursor and radionuclide, as well as the parent and daughter radionuclide does not always occurs in reality. A combination between activation processes and natural decay will occur in most of the cases. Consider figure 2.2 where the activation scheme of ^{60}Co is shown, starting from ^{59}Co.

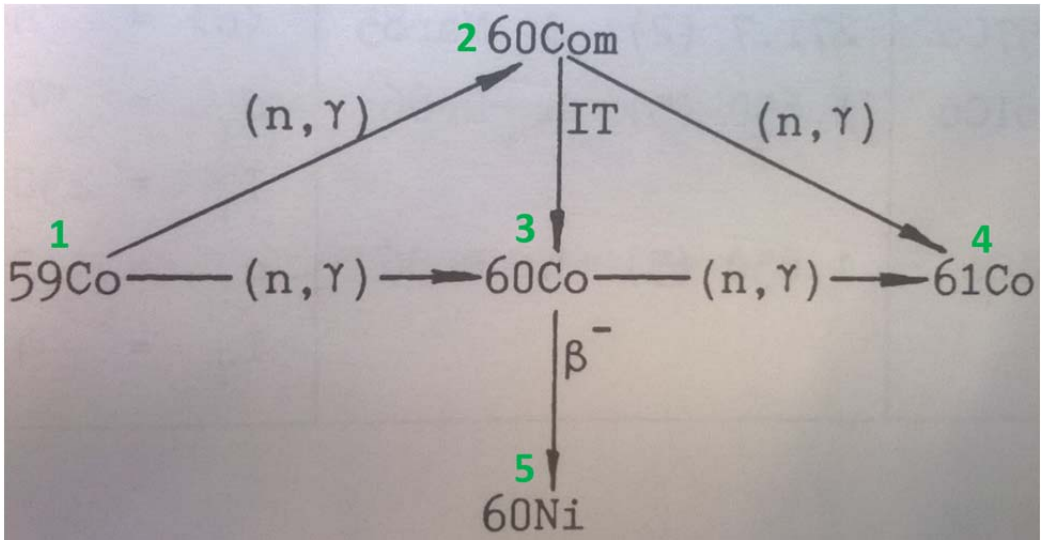

Figure 2.2: Co-60 production and decay chain

^{59}Co is present as an impurity in the graphite but can also be produced from ^{58}Fe.
On the other hand, ^{59}Co is not the only precursor of ^{60}Co. ^{60}Co can be activated by the (n,p) reaction of ^{60}Ni as well as the (n,α) reaction of ^{63}Cu.

The following set of differential equations (2.4) describes the evolution of atoms for each nuclide over time as shown in figure 2.2

$$\begin{cases} \frac{dN_1}{dt} = -\varphi\left(\sigma_{c,1a} + \sigma_{c,1b}\right) N_1 \\ \frac{dN_2}{dt} = \varphi\,\sigma_{c,1b}\,N_1 - \lambda_2\,N_2 - \varphi\,\sigma_{c,2}\,N_2 \\ \frac{dN_3}{dt} = \varphi\,\sigma_{c,1a}\,N_1 + \lambda_2\,N_2 - \lambda_3\,N_3 - \varphi\,\sigma_{c,3}\,N_3 \\ \frac{dN_4}{dt} = \varphi\,\sigma_{c,2}\,N_2 + \varphi\,\sigma_{c,3}\,N_3 - \lambda_4\,N_4 \\ \frac{dN_5}{dt} = \lambda_3\,N_3 \end{cases} \qquad (2.4)$$

When solving these equation, the evolution of the number of ^{60}Co atoms as a function of time is given by $N_3(t)$.

2.2 Waste disposal

2.2.1 Acceptance criteria for surface disposal

The majority of the category A waste consists out of radionuclides with a half time less or equal to 30 years. The major part of the activity is originating from the short lived radionuclides. Except from the short lived nuclides like for instance H-3, Sr-90 and Cs-137, other radionuclides like C-14, Cl-36, Ni-56, Pu-238,Pu-239,Pu-240 can be part of the inventory. Table 2.1 is published by NIRAS in 2008 and is based on safety assessment studies performed by SCK·CEN. It shows the 20 most vital radionuclides for surface disposal in Belgium.

Radio Nuclide	Half life (years)	Ci, max	CAi,max	Radio Nuclide	Half life (years)	Ci,max	CAi,max
H-3	1.2E+01	1.7E+21	1.7E+16	Ra-226	1.6E+03	8.7E+08	4.8E+07
C-14	5.7E+03	6.6E+14	2.5E+09	U-234	2.5E+05	9.0E+09	4.5E+06
Cl-36	3.0E+05	6.0E+13	1.3E+06	U-235	7.0E+08	5.4E+09	4.0E+06
Ni-59	7.6E+04	1.0E+15	7.3E+09	Np-237	2.1E+08	1.0E+10	3.8E+06
Ni-63	1.0E+02	1.6E+15	1.6E+12	U-238	4.5E+09	4.2E+09	4.1E+06
Sr-90	2.9E+01	6.3E+14	6.7E+10	Pu-238	8.8E+01	1.5E+10	6.1E+09
Nb-94	2.0E+04	1.4E+09	6.8E+07	Pu-239	2.4E+04	2.8E+09	3.8E+07
Tc-99	2.1E+05	1.4E+18	2.3E+08	Pu-240	6.6E+03	2.9E+09	2.2E+08
I-129	1.6E+07	2.3E+12	1.6E+05	Pu-241	1.4E+01	1.2E+11	3.3E+12
Cs-137	3.0E+01	3.9E+11	1.3E+12	Am-241	4.3E+02	4.2E+09	1.1E+11

Table 2.1: List of 20 critical radionuclides for surface disposal in Belgium. Concentrations in Bq/m³.[11]

Two criteria will be used to determine the final waste disposal option. First, criterion X is calculated by:

$$\text{X criterion} = \sum_{i=1}^{20} \frac{C_i\,(Bq/m^3)}{C_{i,MAX}\,(Bq/m^3)} \qquad (2.5)$$

Where C_i is the activity concentration of radionuclide "i" expressed in Bq/m³. $C_{i,max}$ is the value listed in Table 2.1 for the corresponding radionuclide and is related to the radiological capacity of the disposal facility. X is calculated for each individual waste package. When X

exceeds 1, then the destiny for the waste package will be geological disposal. When X is smaller than or equal to 1, criterion Y will be evaluated as shown in equation 2.6.

$$\text{Y criterion} = \sum_{i=1}^{20} \frac{C_i\,(Bq/m^3)}{CA_{i,MAX}\,(Bq/m^3)} \qquad (2.6)$$

Where $CA_{i,max}$ is the average activity consumption of the disposal facility for radionuclide i. When Y is lower than or equal to 1, the waste package is suited for surface disposal and uses less radiological capacity than an average package. When Y exceeds 1, then there is a possibility for surface disposal. Its means the waste package uses more radiological capacity than average. The decision tree is shown in figure 2.3

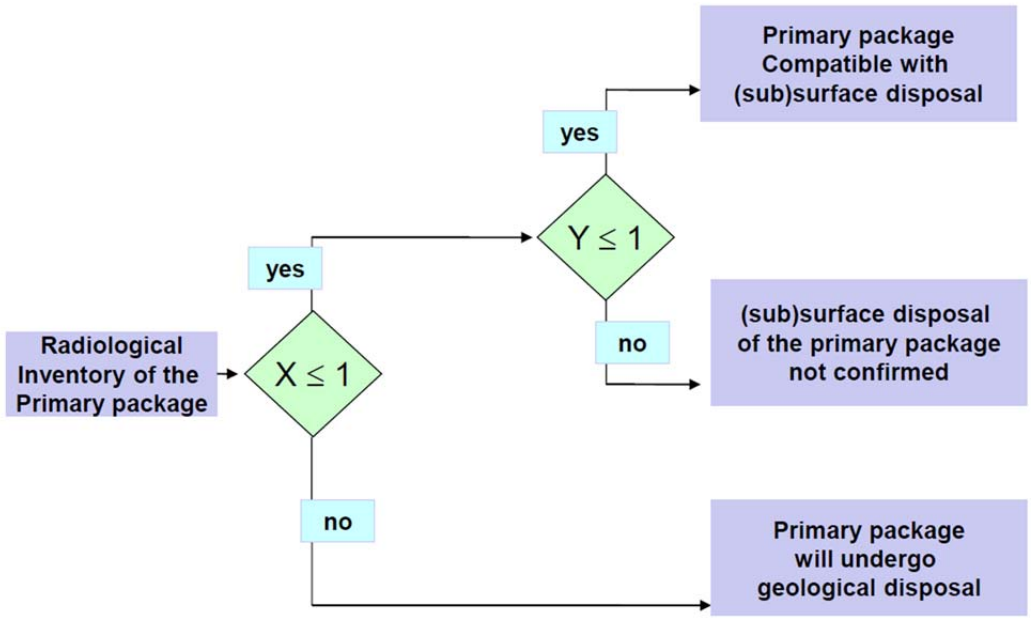

Figure 2.3: Surface waste disposal decision tree. [11]

2.2.2 Surface disposal

Irradiated nuclear graphite is solid waste. The treatment and disposal options for solid waste are based on if the material is compressible or can be burned to ensure volume reduction. Therefore, the waste will require less space for the final disposal. Three types of monoliths are foreseen by NIRAS/ONDRAF as illustrated in figure 2.4. The first type is suited to enclose 4 standard barrels of 400l. The second type for non-standard barrels and type 3 for bulk waste,

like structural materials. Type 2 and 3 are a bit higher, more specific, 5 monoliths of type 2 or 3 stacked have the same height as 6 monoliths of type 1. For that reason, the 3 types can be combined in the same module.

Figure 2.4: The 3 different types of monoliths Cat. A, developed by NIRAS.[12]

Figure 2.5: Future surface disposal site for category A waste in Dessel.[12]

The monoliths are placed inside disposal modules, shown in figure 2.5. These modulus are like concrete bunkers with thick walls of reinforced concrete. Each module measures 27 by 25 meters and can hold about 900 monoliths. In a first phase it is planned to build 20 disposal modules, 2 rows of 10 each. Later on, an additional 14 modules will be constructed.

2.2.3 Geological disposal

When certain volumes of graphite waste exceed the criteria for surface disposal, it will be considered for geological disposal. The geological waste repository will be located several hundreds of meters below the surface. This option is less desirable because of the much higher costs. It requires more advanced enclosure to meet the safety requirements. The objective for geological disposal is the same as for surface disposal: to insulate the waste and protect humans and nature from the possible damaging effects of ionizing radiation. The most challenging tasks is to continue it for tenths of thousands of years without placing burdens on the future generations. The strategy is to concentrate the waste and isolate it from the biosphere. A good geological formation has the ability to maximize the retention and retardation of the radionuclides. At present, no final decision has been made about a location for geological disposal in Belgium. Since 1980, research has been done about the Boom Clay formation. The underground research laboratory HADES is situated at a depth of 225 m on the site of SCK·CEN.[13]

2.2.4 Possible options for irradiated graphite

The final conditioning options for graphite has not been decided yet in Belgium. The obvious option is to include it as bulk waste in monoliths for surface disposal. The benefit for this method is that there are no additional costs besides the disposal costs. No grinding, burning or surpercompacting of the graphite.
A second option is to burn the irradiated graphite, which can be done at the incinerator of Belgoprocess in Dessel. The graphite will first be grinded and later on burned at a temperature of 900°C. The released combustion gasses will be filtered. This technique is very labour and energy consuming, but will reduce the volume of the waste significantly. Burning radioactive waste can cause a volume reduction factor up to 120. The ashes that remain can be cemented in standard barrels or enclosed by vitrification. There need to be mentioned, when considering the incineration option, the specific activity will increase strongly, and therefore may be considered for geological disposal.

3 Methodology

3.1 Introduction

The aim of this study is to make the best possible estimation of the concentration of the radionuclides produced in the irradiated graphite of the BR1 reactor since the start of its operation in 1957. To accomplish this, all the information and computer tools available at SCK·CEN in Mol will be used. The so-called "activation code" ALEPH [10] will be used. Using the acceptance criteria for surface disposal as explained in section 2.2.1 the categorization of the graphite waste of many graphite samples can be done.
It is expected that all the graphite will be suitable for surface disposal based on the low thermal power and non-continuous operation of the BR1. This will be investigated. Also the possibility arises that some graphite at the very outside could be below the clearance levels and therefore not be treated as radioactive waste.
The computational method has several benefits compared to taking physical samples and analyse them. The costs of analysing the samples is quite high regarding the scientists and equipment required for the job. To be able to have a spatial view of the activity and radionuclides present in the stack, many samples are required which takes time and money. Since the reactor is still operating, only samples can be retrieved from the channels (graphite blocks with a hole in) where no fuel is loaded. Therefore only certain locations are accessible. Taking samples of the graphite B without holes at the outside is not possible.
Finally, with this model, the burn up of the fuel will be simulated at the same time. With the data retrieved from the simulation, is it possible to estimate the radionuclide concentrations in the fuel rods and show the burn up of the fuel in function of the time. However, due to time restrictions, it was not possible to analyse the results and discuss them in this work. In order to have a valid computer model and have confidence in the results, physical measurements for comparison are necessary. The measurements used for comparison date from 2011.

It needs to be kept in mind that this is not the final characterization which will serve as the final verdict when dismantling the reactor. First of all, the available samples have only been analysed for a few radioisotopes while the most important ones like Cl-36, C-14 and H-3 are missing. Therefore it is not possible to validate the computer model for 100%. Also the samples were taken in one and the same channel and all of them in graphite A.
There needs to be noted that the methods to analyse irradiated graphite for volatile substances at SCK·CEN have been improved significantly during the past few years.
Therefore, future sample analysis will be of higher interest and will allow the analysis of more nuclides with lower detection limits. A concise overview of the workflow is illustrated in figure 3.1

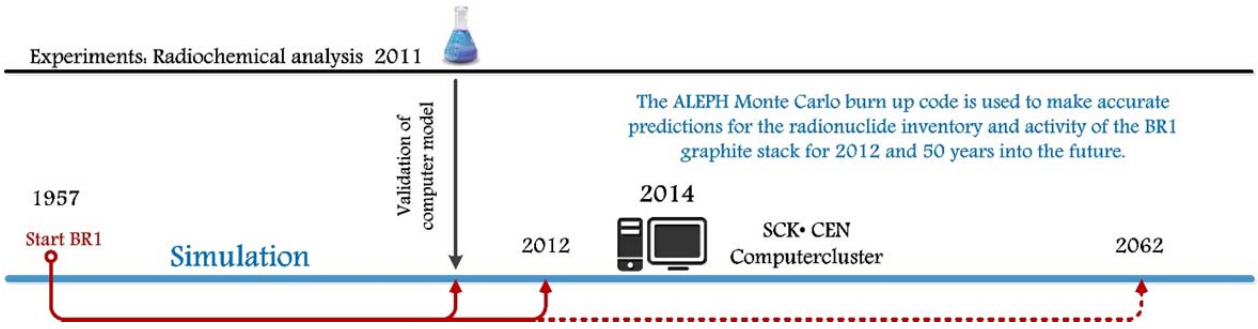

Figure 3.1: Concise overview of the project workflow.

3.2 ALEPH

The activation calculation becomes very complex due the fact that the concentration of activation products present in the BR1 graphite depends on several parameters.
For this reason, advanced computer codes are required. The computer code which has all the potential to perform the requested calculations is ALEPH[10]. A concise calculation data flow of ALEPH is shown in figure 3.2.

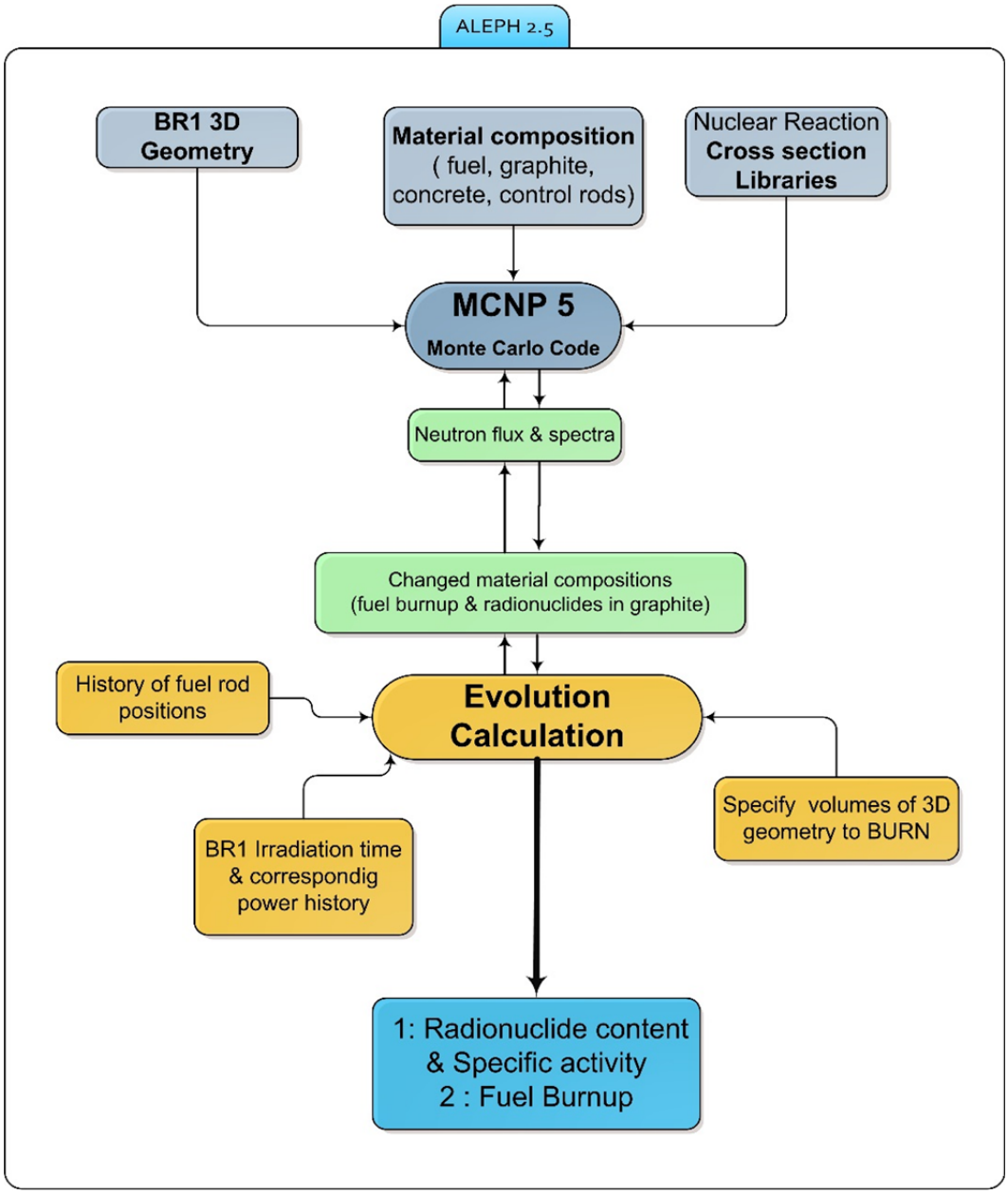

Figure 3.2: Data flow in ALEPH 2.5

ALEPH is a coupling between MCNP (Monte Carlo N-Particle code) and an evolution part developed at SCK·CEN since 2004. MCNP is a standalone certified and well known Monte Carlo code, developed by The Oak Ridge National Laboratory(ORNL) in Tennessee, the USA[14]. An interesting detail to mention: the ORNL hosts the Titan supercomputer which is currently the world's second most powerful computer.

During the last decades, Monte Carlo methods have been used in all kind of nuclear applications. One of them is to simulate the best shielding in a complex geometry to keep the irradiation exposure for workers as low as possible. For this study, the Monte Carlo technique will be used to simulate the neutron fluxes and spectra. In both cases, the trajectories of individual particles are simulated. Simulated means that for a large number of particles, the trajectories are predicted based on probability distributions. These probability distributions are based on theoretical calculation and experiments. The basics are pseudo random numbers, generated by algorithms on the computer. The final results is achieved by taking the average of all the individual simulations. The statistical uncertainty is reversely proportional with the number of simulated particles.

However, problems can also be solved analytically, by solving the differential equations according to the rules of mathematics. This is possible for simple geometries but too complicated for real and complex geometries like the one of the BR1. These geometries can be used easily with Monte Carlo (MC) techniques. However MC techniques are not capable of providing an exact solution for the problem, but are rather an estimation with corresponding uncertainties. Another consequence of using MC technique is that these require huge amount of computer time when requesting very small uncertainties.
To summarise, the major differences between MC and deterministic or analytical techniques are: MC techniques provide an approximate solution to an exact representation of the problem, while deterministic techniques give an exact solution to an approximation of the problem.[14]

ALEPH has the ability to calculate the change of material composition due to nuclear reactions. In our case, ALEPH will be used the model the material composition changes of the graphite as well as the BR1 fuel. In order to compute the radionuclide inventory and activity values, input data is required, as shown in figure 3.2.

First of all the BR1 3D geometry is used. It is an almost identical representation of the actual reactor. The BR1 model is explained in chapter 4. For each material used in the BR1 model, a material composition is defined. Both the 3D geometry and material composition are defined in the input file, which is in fact a large text file. The material composition consists out of all the nuclides and corresponding mass fraction or atom fraction present in that material. The implementation of the impurities present in the non-irradiated graphite is modified in this section of the input file. Nuclear data from cross section library ENDF B.VII-1 was used. The first part of the calculation is the MCNP Monte Carlo part. MCNP is a time independent code and is used to simulate the neutron energy fluxes. These fluxes are calculated for each defined sub-volume with related material inside the geometry.

The results are forwarded to the evolution calculation or activation calculation. As illustrated in chapter 2, the production of radionuclides is dependent on the neutron flux and energy values. In contrast to MCNP is this calculation time dependant.

The lines of code to perform the evolution calculation are added on top of the MCNP input file. First the volumes which will be used in the evolution calculation need to be defined. These need to be of course already be present in the MCNP 3D geometry. The irradiation history is defined in the input. A distinction is made

3.3 How the program works

ALEPH is the Monte-Carlo burn-up code used for calculating the materials composition changes in the graphite as well as the fuel during the lifetime of the BR1, and possible up into the future. The current version used is ALEPH 2.5.2. The MCNP Monte Carlo part is a time independent code, while the evolution part is time dependant. In the first phase of a simulation, the neutron fluxes and corresponding spectra are calculated by MCNP. The flux and spectrum values are calculated for each defined sub-volume with related material inside the geometry. Each energy spectrum consists outs of about 116,000 energy values. Using these spectrums to calculate the corresponding reaction cross section is to computational intensive. Therefore, spectrum averaged reaction cross sections are calculated by ALEPH for each nuclide in the material, for each reaction, for each material at each time step. For this reason the evolution part is a one-group depletion code. Confidential tests have shown that using a spectrum of about 116,000 energy values or groups does not have a big improvement in reaction rates compared to the spectrum averaged cross section σ_{av}, which is calculated by equation 3.1:

$$\sigma_{av} = \frac{\int_{E_1}^{E_2} \sigma(E)\varphi(E)d(E)}{\int_{E_1}^{E_2} \varphi(E)d(E)} \qquad (3.1)$$

Where σ (E) is the energy dependant cross section for a specific reaction with a certain nuclide. These values are used from cross section library ENDF B.VII-1. φ(E) is the neutron energy spectrum at a certain location in the reactor core. It represents the fraction of neutron flux for each corresponding energy interval. For the evolution part, no Monte Carlo technique is used. An enormous set of differential equations is solved by the Runge Kutta method RADAU5 solver. The σ_{av} together with φ (from MCNP) are used to calculate the reaction rates of the nuclear activation reactions.

3.4 Inputs for ALEPH – Keywords

Several input keywords are required by ALEPH 2.5 to be able to run the simulation. Some important input keywords are described briefly:

- **BURN**: The material numbers defined in the MCNP geometry that are used "burned" in the evolution calculation. In our case 50 graphite materials and 34 fuel material were used.
- **VOL**: The volume of the cells of the corresponding "BURN" materials (in cm^3). This is required to be able to calculate the neutron flux.
- **IRP**: An irradiation sub step of constant power
- **DEC**: A decay sub step. No neutron flux present in the system, only natural decay occurs.
- **CHM**: Change one material (number) by another material (number)

A part of the BR1 irradiation history input is shown in figure 3.3.

```
75  HIS
76    IRP t 3.9793  h  1790     $ 1957
77    DEC           h  6976  NO $ 1957
78    IRP t 3.8680  h  1437     $ 1958
79    DEC           h  1485  NO $ 1958
80    IRP t 3.8680  h  2873     $ 1958
81       CHM 61 80      $ UNIVERSE 2 loaded: FUEL
82       CHM 63 81      $ UNIVERSE 4 loaded: FUEL
83    DEC           h  2971  NO $ 1958
84    IRP t 3.8699  h  5827     $ 1959
85    DEC           h  2939  NO $ 1959
86    IRP t 3.7693  h  6046     $ 1960
87    DEC           h  2720  NO $ 1960
88    IRP t 3.0909  h  5800     $ 1961
89    DEC           h  2966  NO $ 1961
90    IRP t 3.2377  h  1909     $ 1962
```

Figure 3.3: Part of the ALEPH irradiation history

3.5 Limitations of the code

The computer code simulates a simplified model of the reality.
Because MCNP is a steady state (no airflow, steady geometry in time) computational code some simplifications are made compared to the reality.
The cooling air of the BR1 with a current flow of 10 m³/s blows large amount of air through the channels for cooling. However air contains large quantities of ^{14}N and ^{17}O which can be activated by thermal neutrons and form ^{14}C according to $^{14}N(n,p)^{14}C$ and $^{17}O(n,\alpha)^{14}C$.
In reality the amount of ^{14}C will be higher. On the other side, the produced ^{14}C will not stay in the graphite and will be carried away by the cooling air towards the air filters. So this limitation of the code is no problem.

4 MCNP Model of BR1

4.1 Technical description of BR1

In 1954, the construction of the Belgian Reactor 1 (BR1) was started in Mol. The purpose of the idea behind it was to have a powerful neutron source for producing radioisotopes and be able to perform fundamental research in the nuclear field. Figure 4.1 and 4.2 show the progress of the construction of the BR1.

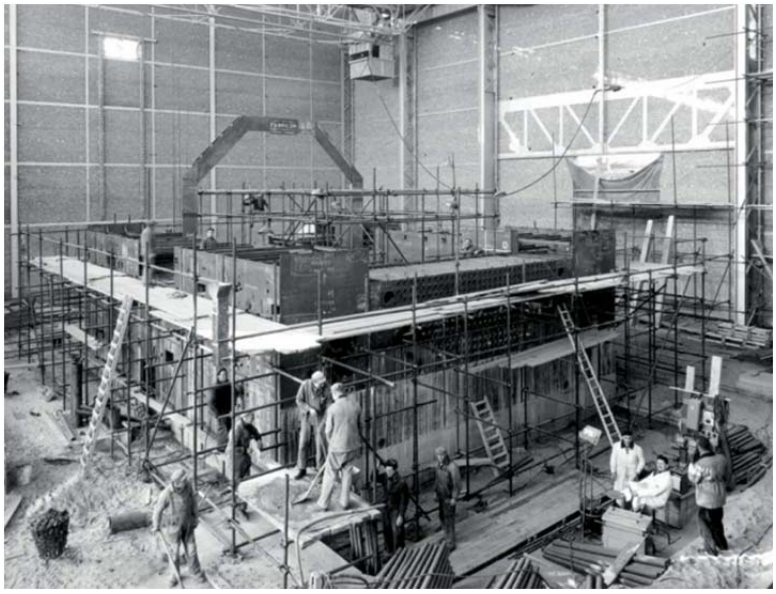

Figure 4.1: Reactor hall: shuttering for the lateral shielding of the BR1, 30th of November 1955.[15]

Figure 4.2: Reactor sides A and D, 28th of March 1956.[15]

De heart of the reactor is the almost cubic graphite massive. It has dimensions of 6.66 m in length and 6.84 m both in width and height. This pile is constructed out of approximately 14000 individual blocks of graphite, with most of them having dimensions of 18 by 72 by 18 cm. [4] These graphite blocks act as the moderator for the fission neutrons (see Appendix D). Some spare blocks of non-irradiated graphite with fuel rods are shown in figure 4.3

Figure 4.3:Several spare virgin graphite blocks of the BR1

To create the exact geometry of the BR1, blocks of additional sizes and dimensions were used. Two types of graphite blocks are used, type A and type B. Type A is of higher quality and is the moderator in the reactor, its mass density is 1.72 g/cm³ and contains 0.4 ppm boron. Graphite B has a mass density of 1.65 g/cm³ and 1.8 ppm boron content. It has the highest mass density and the lowest concentration of impurities. Graphite A quality is located at the center, within a radius of 2.6m. This border is sharp-edged like the graphite blocks were stacked. In the longitudinal direction graphite A ranges from 2.52 m at the back to 2.52 m in the front. Outside the 2.6m radius, graphite B is used. For the first 81 cm at the front and the back of the pile, graphite B was used.[4]
Figure 4.4 shows the BR1 scale model with visible graphite pile.

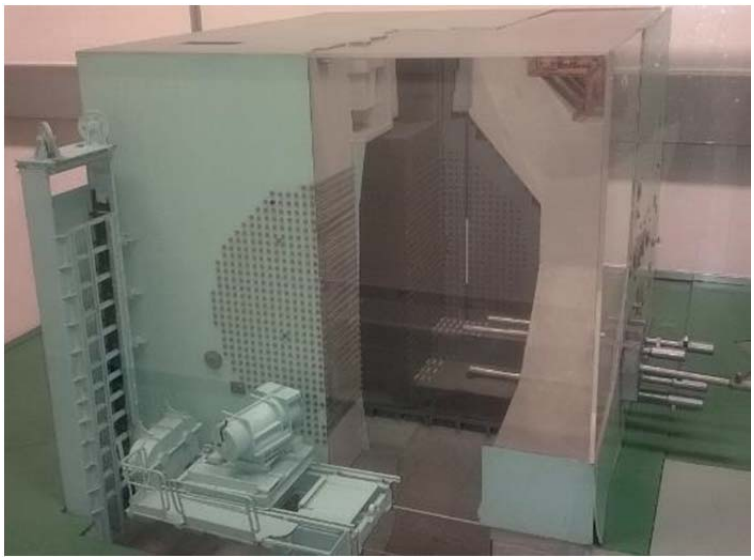

Figure 4.4: Scale model of BR1 with visible graphite pile.

The total mass, graphite A and B together is 492 tons. From the front view (side A) the openings of the 829 fuel channels can be seen, shown in Figure 1.4. A fuel channel is a square hole of 5 by 5 cm at an angle of 45° for the total length of the graphite pile, visible in Figure 1.3. Inside these openings, the 23 fuel rods are placed, next to each other. These cylindrical rods are touching the graphite at 2 contact lines. With this shape, air can pass over and under the hot fuel rods to cool them. The fuel rods have a length of 20.4 cm and a diameter of 2.54 cm. The mass is 2030 g containing 1950 g of natural uranium. Therefore the BR1 is of the reactor type graphite moderated air cooled natural uranium reactor. At the current configuration 552 out of the 829 fuel channels are loaded which corresponds to a total of almost 24.8 tons of natural uranium. The shielding of the graphite pile to protect the workers outside the reactor is a 2.1 m thick concrete structure around the pile. The density of the concrete structure is 3.4 g / cm^3 and is capable of reducing the intensity of the irradiation by a factor of 10 million [4]. Experiments can be performed on and around the reactor during operation while keeping the received personal dose far below the legitimate limits. Between the graphite pile and the concrete, an air gap of 1 m is present for the air cooling of the reactor. This is accomplished by a large turbine which is placed behind the reactor in the cooling circuit. Hereby, fresh air is aspirated trough filters inside the building, moving through the fuel channels. The heated air can reach temperatures up to 90°C. It passes through the fan, and finally leaves the system through the chimney.

4.1.1 Reactor usage

During its early years, the reactor was most of the time in operation for the production of medical radioisotopes. But since the start-up of the BR2 (Belgian Reactor 2), which is more advanced and has higher neutron fluxes, up to 10^{15} n.cm^{-1}.s^{-1} compared to the 10^{12} n.cm^{-1}.s^{-1} of the BR1, the production of medical radioisotopes stopped in 1964.
On the side/top of the reactor, experimental channels with high neutron reference fields are available to calibrate neutron radiation detectors.
In the thermal column, dosimetry measurements are performed. When evaluating a new type of dosimeter, the BR1 acts as the neutron source to deliver the desired dose, depending on the location in the reactor and the irradiation time.
Neutron Activation Analysis (NAA) is a very precise and accurate non-destructive technique to determine the composition of a certain material. By irradiating unknown samples by neutrons, radioactivity is induced in the samples due to nuclear reactions (n,γ) or (n,α) for instance. Afterwards, the radioactivity is measured and is used to determine the elements and their concentration in the samples. One of the major advantages of this technique is the very low detection limit. This activity of the BR1 stopped in 2010.
Besides the research and experiments, the BR1 is often used for training young engineers or is visited by university student from Belgium.

4.1.2 Future activities

The exploitation costs of the reactor are very low. These costs includes several things. First of all the fuel costs. Since 1956 only 1.4 tons of fresh fuel has been replaced in the center of the core, compared to the total of about 24 tons, the reactor is using 95% of its initial fuel. At the current working regime of a few hours a day, depending on the demand of SCK·CEN or external clients, it is estimated that the current fuel can cover the next 50 years of operation. The supervision team, consisting out of 5 persons and the maintenance work expenses are limited. While the safety accommodation meets the standards of today
the BR1 has still a bright future within sight. Some important parameters like temperature, airflow and radioactivity of the released cooling gasses are displayed on a pc monitor, to make the handling and control easier. When the reactor is still useful for a variety of activities with a limited of expenses, there is no reason to shut it down in the near future.

4.2 Irradiation history & fuel configurations

4.2.1 Available information

The irradiation history is an important parameter for the activation of the impurities. The higher the thermal power of the reactor, the higher the neutron flux, and regarding the formula for the reaction rate, this will translate in a higher production rate of radionuclides. The same applies for the irradiation time. The thermal power of the BR1 has been measured since the beginning. It is expressed as integrated power (MWh) where one MWh equals the energy equivalent of 3.6 GJ. The BR1 became critical on May 11th 1956 but from that moment until the end of 1956, the reactor had been used executively for testing purposes. Since the real start in 1957 until the end of 1960, the reactor was operating at a thermal power of about 4MW. From 1961 until the end of 1964 the reactor operated at a thermal power between 3 and 3.5 MW. It was working according to periods of two weeks followed by several days of shut down.
Since 1965 the reactor works at another regime, at about 700 kW_{th} during several hours a day. The explanation of the big switch in working regime is that the BR2 (Belgian Reactor 2) became operational and took over some important tasks of the BR1. The BR2 is a more advanced research reactor and is capable of producing neutron fluxes up to 10^{15} n/cm².s. Currently, the BR2 is still the most important facility of SCK·CEN.

The accumulated integrated thermal power in GWh of the reactors lifetime is visualised in figure 4.5. It is shown that the irradiation majority took place before 1964.
The integrated power of the reactor is fluctuating heavily from day to day because the research reactor works according to requests in contrast to a nuclear reactor for electricity production. Even from month to month there is still much variation as illustrated in figure 4.6. We are more interested in the yearly average power. First of all, a monthly time step will have no big improvement regarding the activation calculation compared to a time step of one year. Secondly, the ALEPH code calculation will require too much time when using a monthly time step over a total period of almost 60 years what results in over 1300 evolution steps.

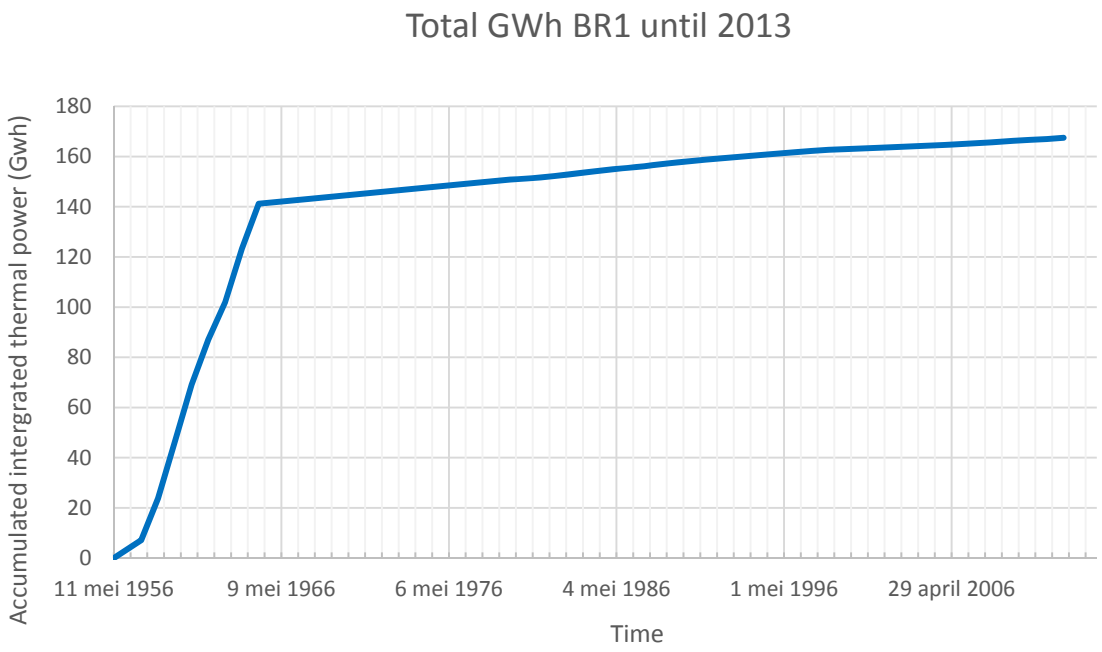

Figure 4.5: Accumulated thermal power (GWh) from start up to 2013.

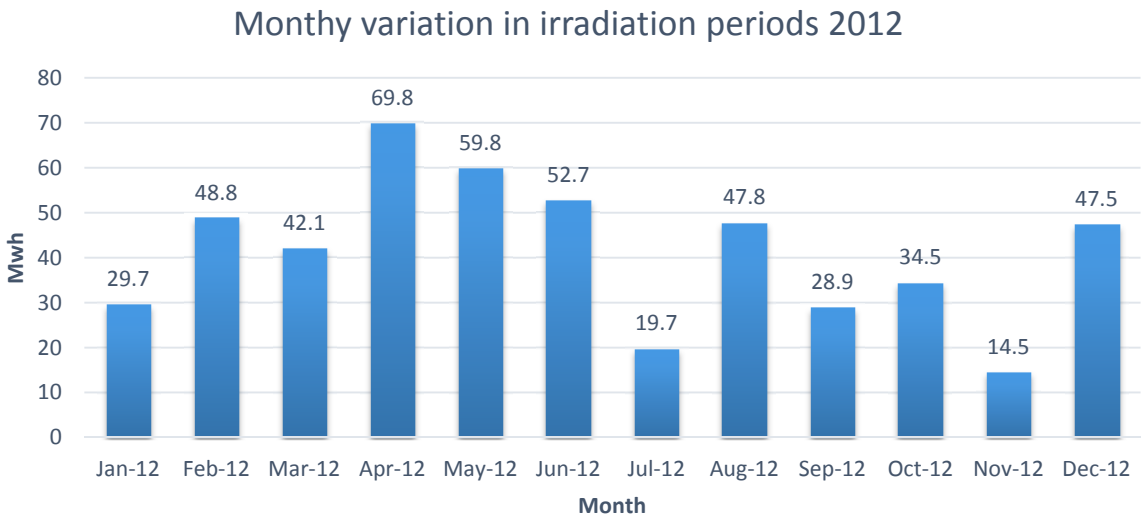

Figure 4.6: Monthly integrated power variation for BR1 in 2012.

The initial procedure to partition the graphite zones was based on the neutron flux distribution of the current fuel configuration, with 552 loaded fuel channels, each with 23 fuel rods. These channels are loaded starting from the center of the core, radial expanding with the exception of a few empty channels. The fuel in these channels have been unloaded in the past

years. This procedure was not justified, due to the fact that the number of loaded fuel channels has changed during the operation time of the BR1. Since the aim of this work is to simulate the graphite activation during the lifetime of the reactor, it is necessary to take the fuel configuration changes into account.
To have a better understanding of the fuel loading patterns, several official and historical documents about the BR1 have been consulted[4,16,17]. These documents, most of them in French were available in printed or pdf (scanned) version. This was certainly important information to include into the computer model. There needs to be understood that the first configuration consisted out of 501 fuel channels loaded. This configuration was used from June 1957 until the 25th of April 1958 [4]. It was assumed that the BR1 started its operation in January 1957, as recorder in the irradiation power tables. Therefore, the first period with the 501 configuration was defined from the first of January 1957 until the 30th of April, as used in the computer model. There were some uncertainties of the order of magnitude of a few days difference, but this will have negligible impact.

The second configuration of 520 fuel channels started in May 1958. Afterwards it has been increased to 569 fuel channels, however the exact date could not be traced back. In the safety report part 3[17] was noted that in May 1962, all the fuel was unloaded and temporary stored in an nearby storage facility. This was done to anneal the graphite and remove all the stored Wigner energy in the graphite for safety reasons. The annealing period took 4 day , but nothing was said about the time required for loading and unloading the almost 12000 fuel rods.

Another change of fuel occurred in 1967. The most irradiated fuel was unloaded and replaced by fuel rods from the most outside region (periphery). This highly irradiated fuel had a mass of 1.4 tons and occupied a region in the core with a diameter of 1.8 m. The fuel rods itself from the periphery were replaced by fresh fuel rods. The unloaded fuel has been reprocessed by EUROCHEMIC in Dessel at that time. Currently EUROCHEMIC doesn't exist anymore and is part of BELGOPROCESS.[17]

When combining all the available information from documents, reports, fuel rods fiches from the BR1, the following six periods have been distinguished (Figure 4.7):

- The first period (1957-1958), 501 fuel channels loaded
- In Mai 1958, 520 channels were loaded.
- In Mai 1962, all the fuel was unloaded. There had been assumed that the whole month there was no irradiation and additionally that the fuel was replaced at the same position after the annealing. The next assumption was the date for the transition from 520 to 569 fuel channels. It looked obvious that it took place after the annealing, so from June 1962.
- After February 1967, the reshuffling of the central spent central fuel took place while the number of fuel channels, 569 kept unchanged.
- The following period started on the 4th of February 1983.
  (1st of February used in the computer model). At that time, the eight fuel channels around experimental channel Y4 had been unloaded.
  The eight channel numbers :
  D1.1 – D2.2 – D1.2 – C0.2 – D2.3 – D.1.3 – C0.3 – D1.4.

  An additional simplification has been made to also unload channel A1.2 at this time. In reality was channel A1.2 unloaded in 1975 as listed on the fuel channel identification card. This was done because it is only one channel which is nearby the other eight channels. In the computer model, the fuel will be present 8 years longer than in reality. Therefore a small overestimation is made regarding to the activation of the graphite.
- The last transition took place at 23th of September 1994, almost 20 year ago. At that time, the eight fuel channels around experimental channel Y6 has been unloaded. Y6 is empty with the dimensions of a square of 24 by 24 cm.
  The channel numbers are: C2.1 – C3.1 – C4.1 – C2.2 – C4.2 – C2.3 – C3.3 – C4.3
  Channel C2.3 is an important channel: it is the channel where the samples were taken in 2011 for gamma spectrometry analysis. For instance, if this unloading was not taken into account in the computer model, the difference between the radiochemical analysis would be larger and attributed this to the impurity list, while in fact it’s not.

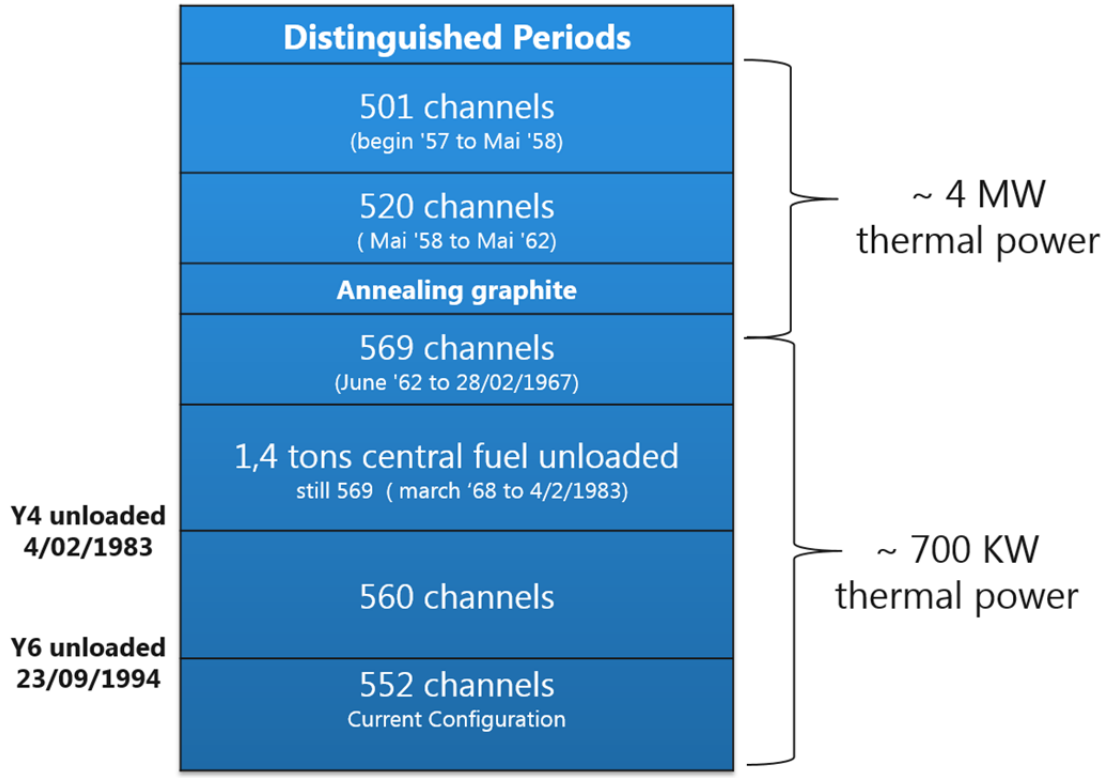

Figure 4.7: Distinguished periods during operation of BR1.(based on [4,16,17])

A remark need to be made:

In the confidential archive of the BR1, there is a history for each fuel channel and each fuel rod, logged on a paper card. The fuel channel cards include the arrangement of the fuel rods by their ID numbers. This is shown for each date when a change has been made. A change could be the combination of unloading certain fuel rods, adding fuel rods or replacing them. The fuel rod ID cards contain information about the channel number and positions with corresponding date during their lifetime. First the periods had been distinguished by the "old French documents" and later on, some important facts were checked with the cards in the archive. The most important fact was the axial positions of the fuel rods during the fuel reshuffling in 1967.

Fresh fuel has been added at the outside during the years for compensating the decrease of the reactivity, due to the burn up of the central fuel. The reason for unloading the fuel around experimental channels Y6 and Y4 was to have a more thermal energy spectrum in those channels.

4.2.2 Implementation of information

Once all the required information was collected, a “BR1 fuel loading map” was made. First is was made in Microsoft Excel to be later on implemented in ALEPH. It represents the front view of the reactor as illustrated in figure 4.8. The four quarters are labelled by A, B, C and D. The yellow squares represent graphite A while the green one represent graphite B. First there is the 501 configuration: All the channels which are filled by fuel in this configuration are labelled with the number 1. A symmetrical loading pattern was used, starting from the center. At a given point, 496 channels were loaded and 5 more needed to be loaded to achieve 501. This cannot be done fully symmetrical, therefore the 5 remaining channels were filled in quarter A as illustrated by a thick contour.

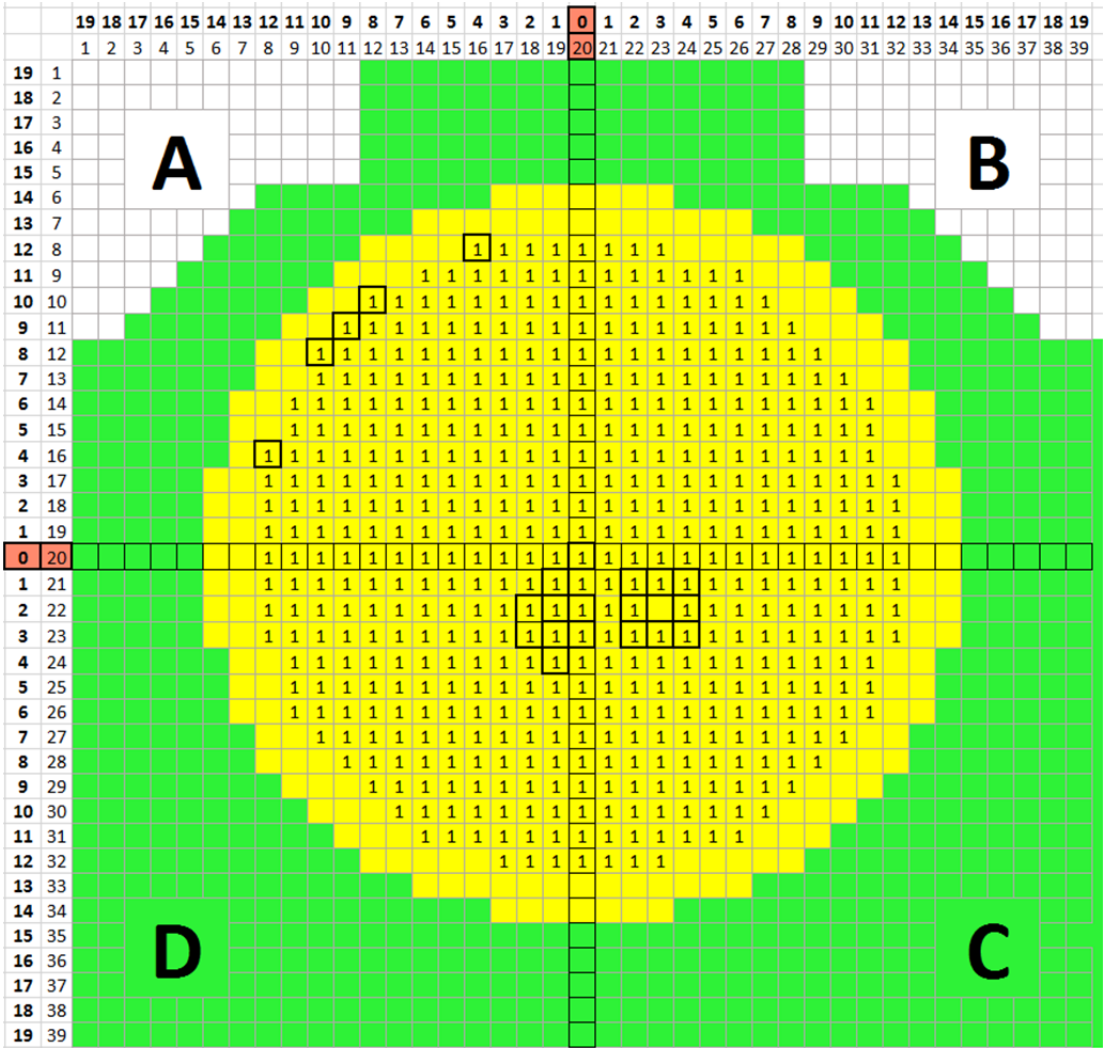

Figure 4.8: Initial 501 configuration.

In the next phase, 19 channels were added to achieve a total of 520. These 19 additional channels got the number 2. This approach has been used for all the configurations. The complete fuel map is shown in figure 4.9. The same number represents fuel channels which share the same irradiation history which implies that all the fuel rods with the same number in the map were loaded, unloaded or rearranged at the same moment.

At first sights, this can look a bit confusing, but it's the best way to represent which channels where changed at the same time. This is a good visual overview and useful to implement the different fuel channel configurations at the corresponding date into the computer model.

The light green squares represent graphite B with holes, while the dark green ones at the outside represent graphite B blocks without holes. All the channels inside, including nr. 10 is graphite A.

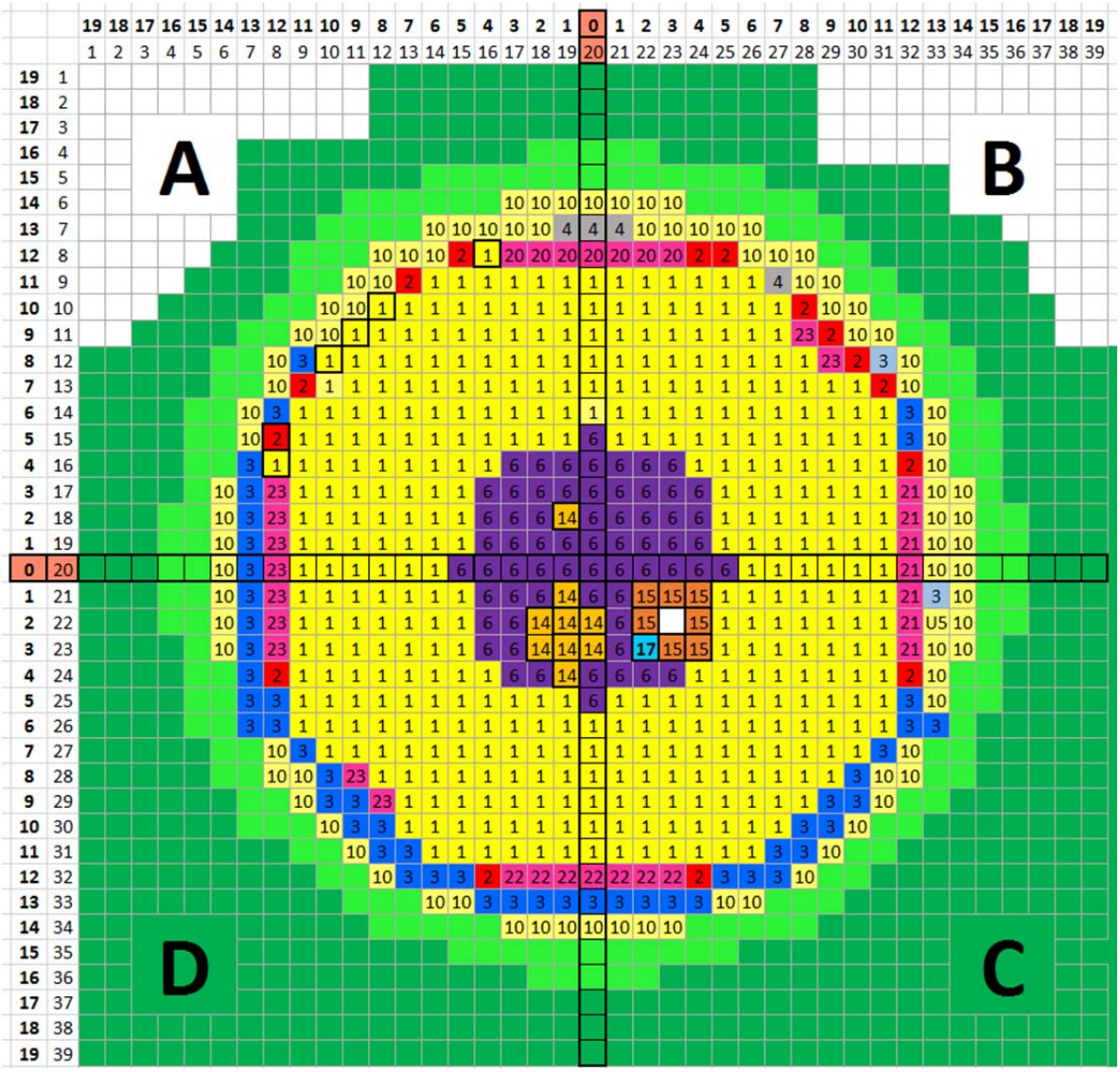

Figure 4.9: Final fuel channel map of BR1

To load the specific configuration, illustrated on figure 4.9:

- 501 channels: Numbers 1,6,14,15,17,20,21,22,23 are loaded with fuel. All the other channels are empty. (January 1957)
- 520 channels: 19 additional channels are filled. The numbers 2 and 4. (Mai 1958)
- 569 channels: nr. 4 unloaded, together with fresh fuel, all channels nr. 3 were loaded. (June 1962)
- Central fuel reshuffling: 9 fuel rods out of the 23 in the 80 central channels, nr. 6, 14, 15 and 17 were unloaded. These positions were filled by fuel of channel nr. 20,21, 22 and 23. Fresh fuel was placed in the channels nr. 20, 21, 22 and 23. (March 1968)
- 560 channels: The 9 channels around Y4 with nr.14 were unloaded. (February 1983)
- Current 520 configuration: The 8 channels around Y6, with nr. 15 and 17 were unloaded. (September 1994)
- Channel Nr. 17 is channel C2.3, were the samples were extracted, for this reason it has a unique number.

Changes in the geometry need to be incorporated in the input file, which is in fact a big text file. In order to check if the changes are made in the correct way, a plot of the geometry can be made by MCNP as shown in figure 4.10. This is a slice of the front, through the center of the reactor.

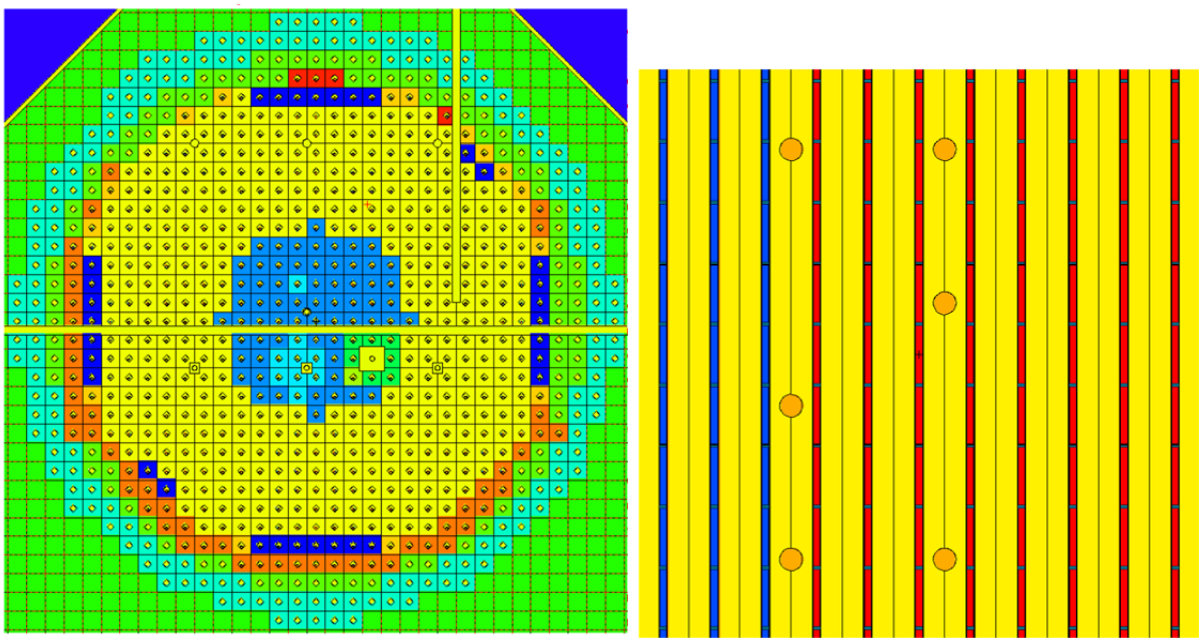

Figure 4.10: Channel zone partitioning in MCNP plotter (left) and cross section of channels with fuel rods (right).

When zooming in, there can be seen that the fuel of different zones also have different colours. This is correct, because different materials have been assigned to these fuel rods. At the beginning, all the fresh fuel has the same composition, but during the irradiation of the BR1 the material composition will change differently in time, corresponding to the location in the reactor core.

Figure 4.11 displays the irradiation and decay periods of the reactor at the corresponding power. This is the visual representation of how it is implemented in ALEPH. Only the time window from 1957 to 1967 is shown. The area of each bar represents the integrated power or energy. In reality there was a day to day variation but in this case there was opted for intervals of one year, except when a fuel configuration change took place, then that year was split into 2 intervals. Each year consist out of a irradiation period and a decay or cooling down period when the reactor was not operating. Each irradiation period is represented by a bar. A yearly time interval was necessary to perform the number of activation and decay calculations (about 140) from 1957 to 2012 in an acceptable time span. The different colours represent the different fuel loading configurations of the reactor core as explained earlier and shown in figure 4.7. For instance, the number of fuel channels loaded changed from 501 to 520 after march 1958. Therefor, 2 distinct periods are made, the first one consisting out of 3 months and the second one out of 9 months. The same ratio irradiation time (4310h) to total time (8766 h) in 1958 is preserved for the 2 individual periods.

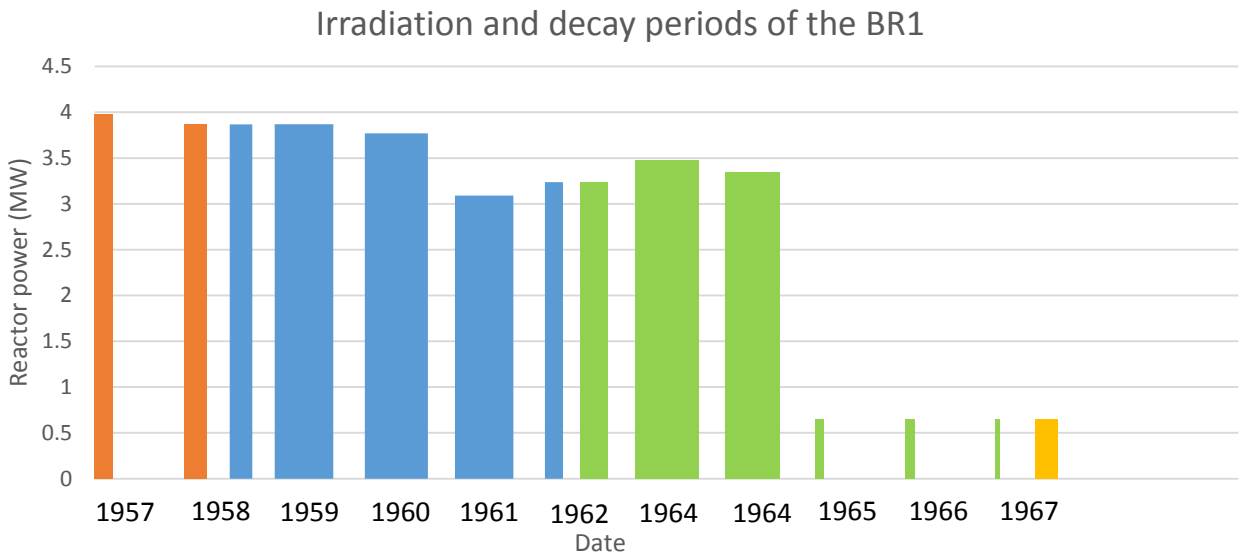

Figure 4.11: Irradiation and decay periods of the BR1 used in ALEPH from 1957 to 1967.(based on [4,16,17])

The much lower regime, both thermal power, height of the bar and irradiation time, width of the bar, can be observed after 1964. As a result, most radionuclides are expected to be produced in the early history of the reactors operation.

When a fuel replacement is carried out, the spectrum and flux is recalculated by MCNP, to update the spectrum and to have a more accurate activation calculation in the next step by ALEPH. This step by MCNP requires between 12 and 18 hours, depending on the number of CPU's and number of particles used. It is skipped when the fuel configuration doesn't change for many years.

4.2.3 Implementation & execution

4.2.3.1 Fuel rods segmentation

In order to correctly model the fuel replacement of the 80 central channels, segmentation of the fuel zone is required. Currently all the 23 fuel rods or slugs are combined together to one volume. The reason is a reduction in calculation time, which is influenced by the number of volumes, for the evolution part of ALEPH. In order to model the displacement as shown in figure 4.12 a segmentation of the fuel in four zones is required. The four fuel zones have a length of respectively seven, two, seven and seven standard fuel rods. A standard fuel rod has a length of 20.4 cm.

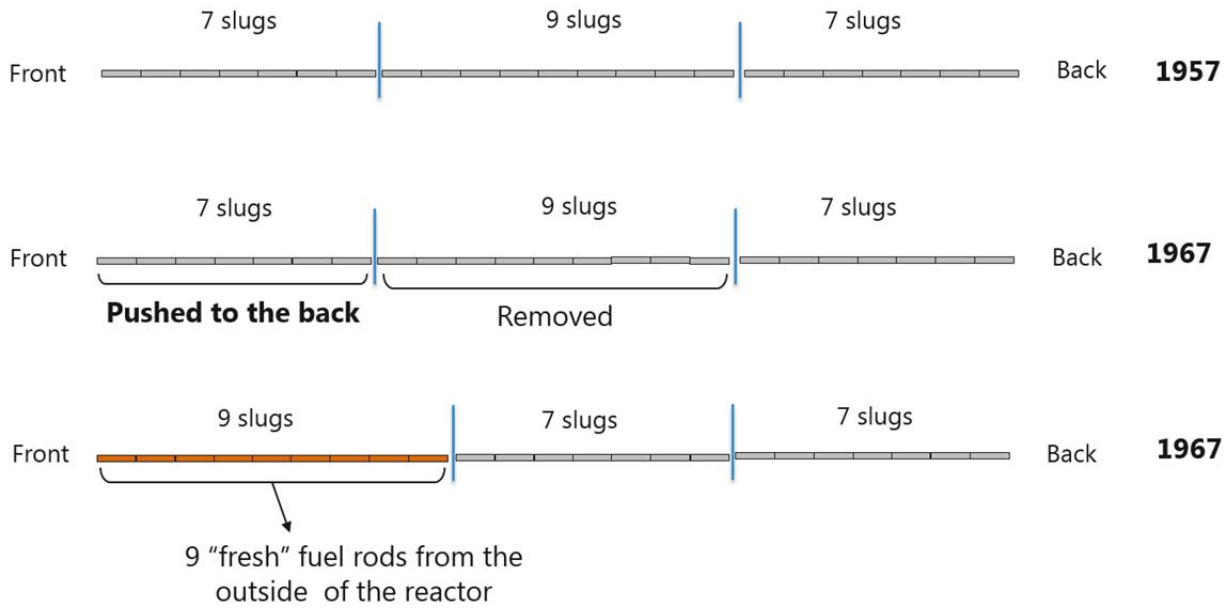

Figure 4.12: The way the fuel was replaced in 1967. (Based on BR1 fuel channel cards of BR1 archive)

When considering the previous map in Figure 4.9, the fuel segmentation is only performed to zones 6, 14, 15 and 17. The reason was that only the fuel rods in these channels were replaced in 1967.

As explained earlier, ALEPH has the ability to change materials. The process of unloading fuel is accomplished by changes the fuel material to air (material with the composition of air). To use this ability of ALEPH in a straightforward way, the fuel was changed to a homogeneous mixture of one material. The new material composition was based on the mass contribution of the individual nuclides. It is straightforward that the current model is a bit less accurate because the real geometrical structure of the fuel rods is not maintained. The modified fuel rod material composition is shown in Table 4.1

Nuclide	Mass fraction
92-U-234	0.00005
92U-235	0.00695
92U-238	0.95787
Al-27	0.03365
Si-28	0.00149

Table 4.1: Fuel rod mixture composition

The speed at which the evolution part can be performed is dependent on the number of materials used and the number of nuclides present in the materials. A material number corresponds to one or multiple cells. Each cell has a specific volume defined by surfaces. Because of the big impurity list of about 230 nuclides, this calculation will take much longer than the average burn up calculation of fuel. One way to keep the calculation time acceptable is by reducing the number of materials as much as possible. Therefore the 23 slugs were combined to one long rod of approximately 492 cm.

4.2.3.2 Graphite segmentation : previous models

The first idea was to segment the graphite blocks “channel wise” in the computer model, and therefore assign a different material number to each volume which was based on the fuel loading history. Each number, as shown in previous Figure 4.9, belonged to a different “graphite burn-up zone”. However this segmentation had some drawbacks. Zone 1 is very large (has a large radial distance). The flux values will differ much between the inside and outside. Also, the central zone, assigned number six is too large. The computer model would average the neutron flux values and as a results the activation products are averaged strongly and the possible border between different waste categories could be vanish. The second drawback related to this method is when calculating the whole graphite structure with all the impurities, it would require too much computer time. (both from the MCNP and Evolution part). Therefore, the new idea aroused to consider several channels of graphite at different radial offsets from the center. Eleven channels were chosen. This is illustrated in Figure 4.13 by the numbers 17, and 29 up to 38.

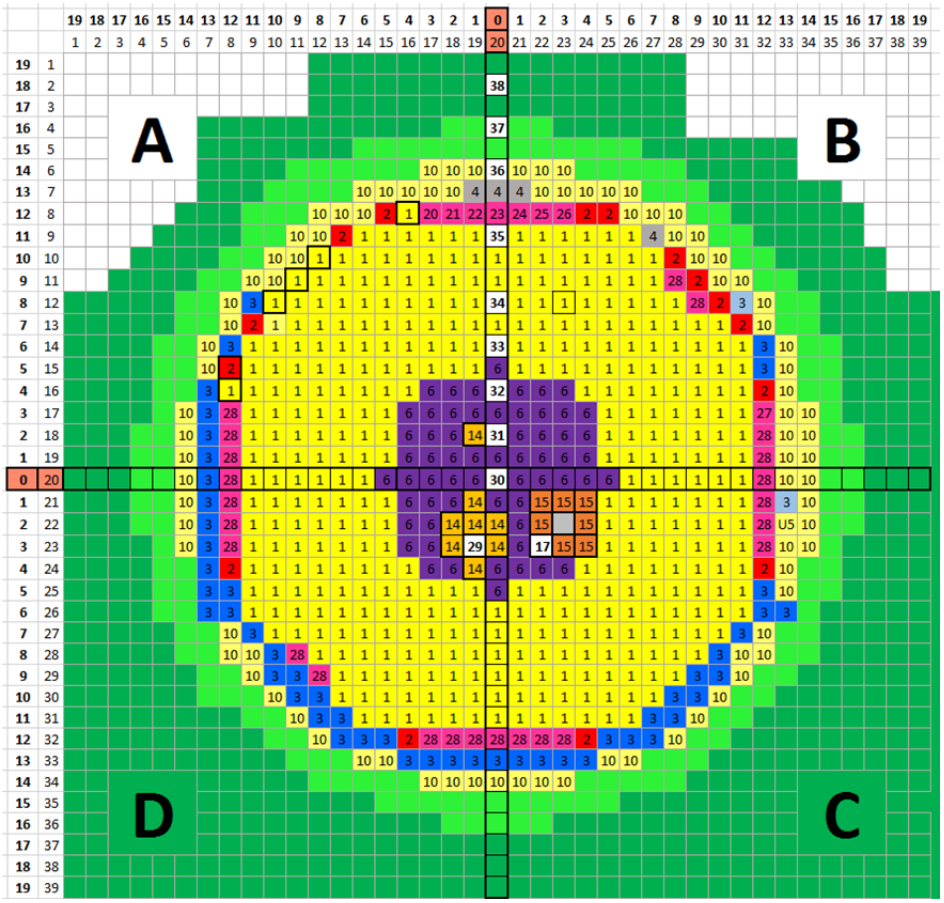

Figure 4.13: The 11 channels (white) chosen to perform the activation calculation on.

Nine channels are located in graphite A, while 2 in graphite B (nr. 37 and 38).
The graphite in these eleven channels contained the impurities while all the other graphite consisted out of carbon with the boron equivalent. When considering these specific channels, the activity levels will be more place dependant and because of that more accurate.

Segmentation in the axial direction is also important. First of all, the neutron flux decreases with increasing distance from the center. Secondly, above the 252 cm in both direction, graphite B is present with a different impurity concentration relative to graphite A. An axial segmentation between graphite A and B is self-evident. Additionally, the zone of 504 cm graphite A is too large and can be subdivided. Figure 4.14 illustrates the axial graphite segmentation.

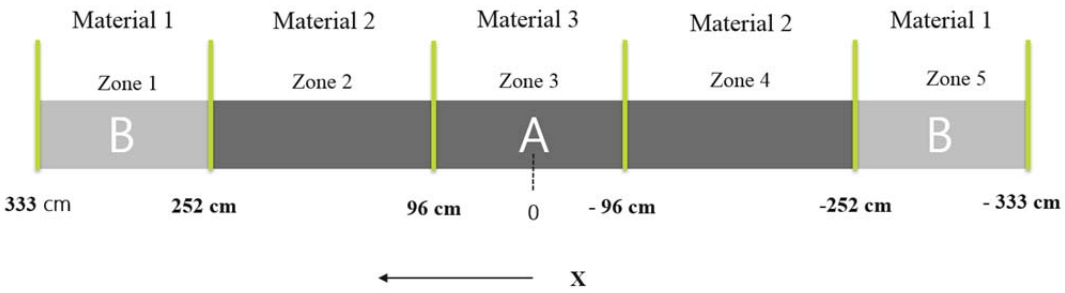

Figure 4.14: Axial graphite segmentation.

The distances of 96 cm were chosen based on the length of the nine central fuel rods (192 cm). Based on the flux distribution of the current 552 channels, it is shown that the flux is quite symmetrical in the axial direction. This observation is used in the computer model to speed up the calculation. More precise, symmetrical volumes are expected to have the same flux values, and are assigned to the same material number like material one and two in Figure 4.14. The materials will have the same flux values calculated and the production of radionuclides is averaged over both zones.

The flux variation in material two was also verified by plotting the axial neutron flux for channel A0.0, A0.5, A0.7, A0.9, A0.11 and A0.13 (Figure 4.15). Based on these values, an additional segmentation of graphite A between 96 cm and 192 cm was made.

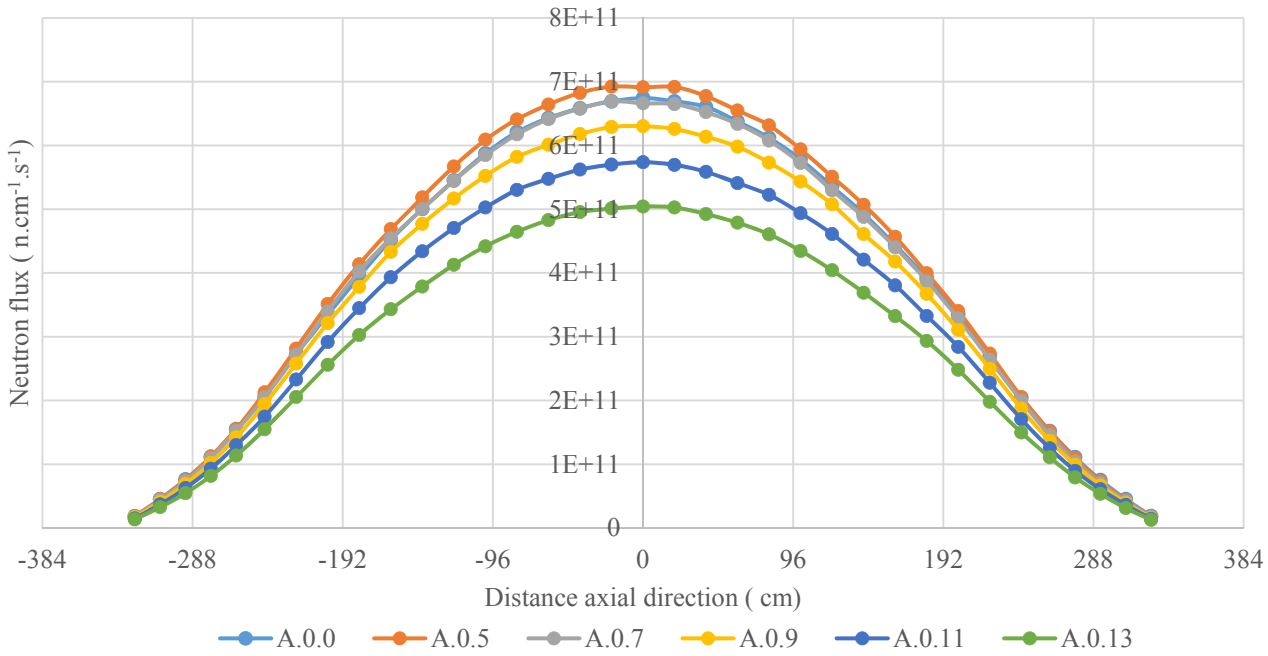

Figure 4.15: Neutron flux in axial direction for different fuel channels, based on current 552 configuration.

4.2.3.3 Graphite segmentation : Final model

In the final computer model, which was the results of improving the previous versions, a different approach was used for the graphite sub volumes. The eleven channels were still used, but small cylindrical volumes were placed inside which contained the complete impurity list. The graphite outside these cylinders did not contain the impurities but only the boron equivalent. The cylinders had a length of 10 cm and radius of 1.5 cm.

These graphite samples were not defined randomly but there position was well considered in the large graphite pile, to be able to observe the difference of variation in neutron flux, spectra and impurity concentration depending on their location. This was done so that afterwards a good idea about the radionuclide inventory and activity levels of the small graphite samples could be obtained. In total 44 samples or sub-volumes were placed, which corresponds to four per channel. Three cylinders were placed in graphite A, with the center of the cylinders at 0 , 120 and 240 cm. The cylinder in graphite B was located at 300 cm axial distance. These were placed at a height of 6 cm regarding the origin of the channel. Figure 4.16 shows a cross section of several channels.

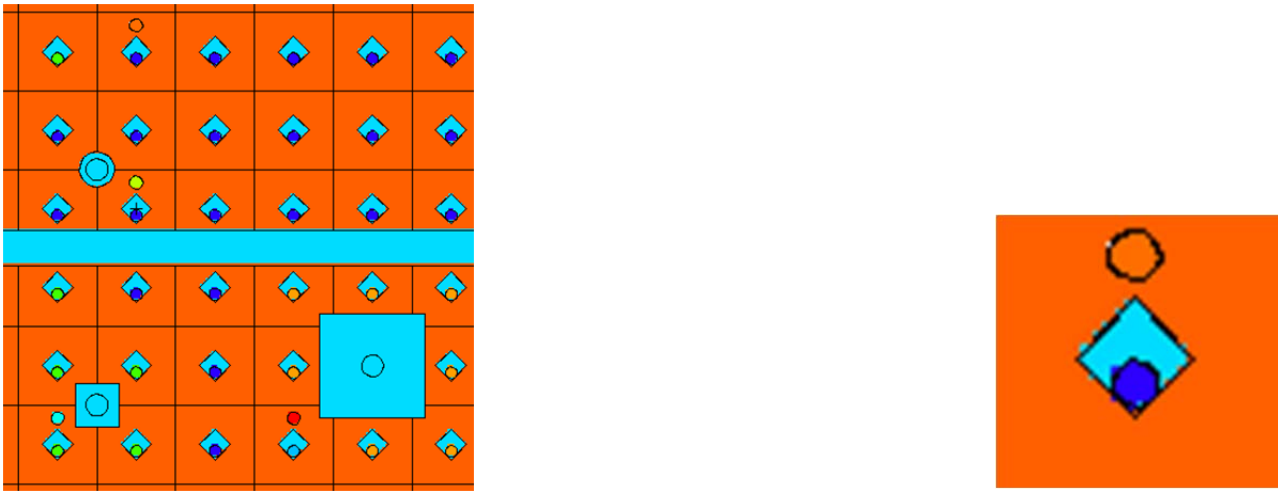

Figure 4.16: Graphite impurity samples, visible as circles in the channels above the diamond shaped air cavities.

The improvement is that the radionuclide inventory and activity is calculated in a very small volume. In this case more precise values could be achieved. Important is that the K_{eff}, the reactors reactivity, will be less influenced. The explanation for the maintained reactivity is that the impurities are only present in these small volumes. Another advantage of this approach is that it's possible when an additional simulation is performed, e.g. with different impurity concentrations for some important elements, only the evolution part needs to be restarted. No MCNP flux and spectra calculations are required because the impurities in the small volumes have slight impact on the neutron spectrum.

This is not really correct, because except for the graphite samples and impurity volumes, the complete graphite structure contains boron. However, this material is not "burned" by the evolution calculation. Boron is a strong neutron absorber but in the computer model it is not reduced over time due to nuclear reactions.

4.2.3.4 Graphite segmentation : measured samples

This section is related to the results from the gamma spectrometry analysis in 2011.
In 2011, 3 samples, B, D and E were taken from irradiated graphite A quality, located in channel C2.3, which is not loaded by fuel. The axial position of the samples is illustrated in Figure 4.17 and the samples in Figure 4.18. The left corresponds to side A which is the front of the reactor while the right corresponds to side C or the back side. The axial positions were 447cm, 547cm and 597cm with respect to side A. The report is from 20 June 2011 with the reference date of 20 may 2011. The equipment to take small samples from the graphite blocks has a hemispherical shape. The mass of each subsample was 1.2g. Sample B was taken at the right side, while samples D and E were taken at the left. The analysis was performed at the laboratory for gamma spectrometry at SCK. The report is added in Appendix A.

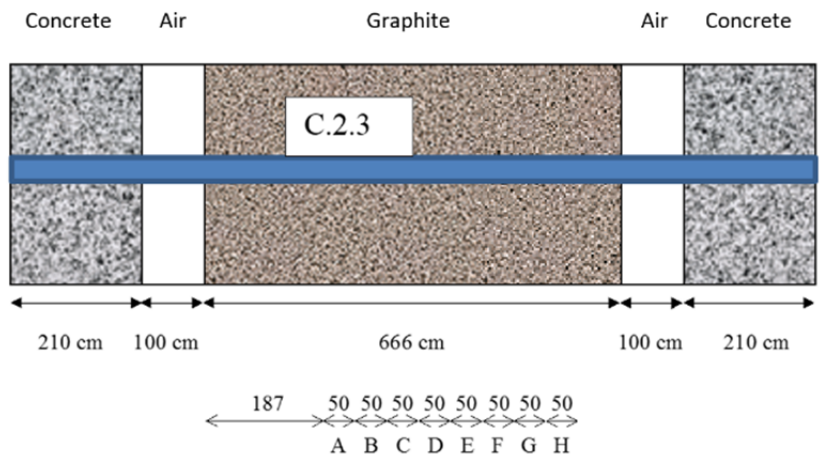

Figure 4.17:Axial positions of the samples in channel C.2.3

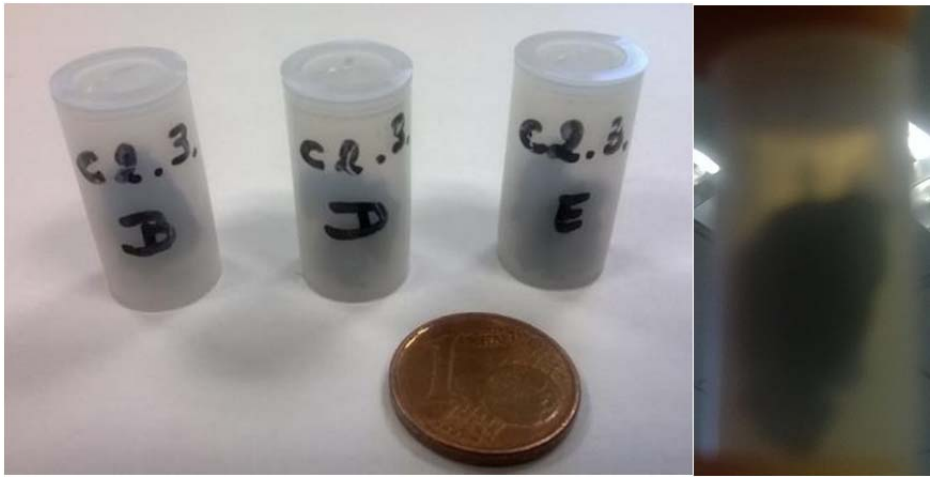

Figure 4.18: Irradiated graphite samples B,D and E.

In order to use these results to validate the computer model, more specific the used impurity composition and other assumptions/simplifications that were made, it is crucial to extract the output from the computer model at the exact location where the samples were taken. Three hemispherical volumes were created in the computer model to represent the graphite A sample locations. Sample B was taken at the right side, while sample D and E at the left side (Table 4.2).

Channel	Position	Distance from Face A (cm)	Side
C.2.3.	A	397 /	Right
C.2.3.	B	447	Right
C.2.3.	C	497/	Right

C.2.3.	D	547/	Left
C.2.3.	E	597/	Left
C.2.3.	F	647/	Right
C.2.3.	G	697/	Right
C.2.3.	H	747/	Right

Table 4.2: Axial positions of the graphite samples in channel C2.3.

The position, regarding the x and y distance of the hemispherical volumes is unknown. It was opted to place the center of the hemispherical base at the x and y distance exact in the middle of the channel wall, at 1.7678 cm. This is illustrated in Figure 4.19. The implementation in the geometry in shown in Figure 4.20.

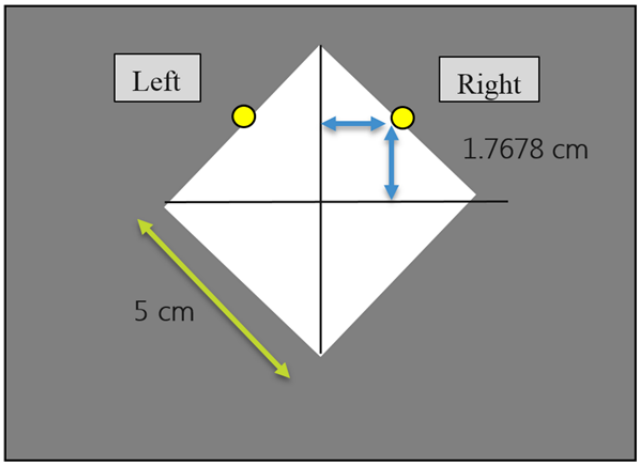

Figure 4.19: Position of the samples used in the computer model.

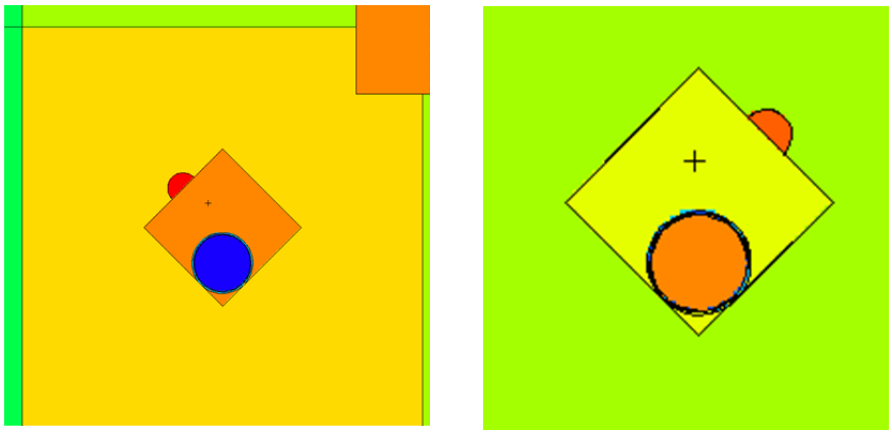

Figure 4.20: MCNP plot of red hemispherical samples in channel C2.3, left and right.

The correct axial position was not so well defined, it could be interpreted in 2 ways as shown in Table 4.3. The reason was a difference in distance between Figure 4.17 and Table 4.2, which was the only information available and didn't match exactly.

Distance to side A of graphite pile		
Sample	**Method 1**	**Method 2**
B	187 cm + 50 cm = 237 cm	187 cm + 50 cm + 25 cm = 262 cm
D	187 cm + (3*50 cm) = 337 cm	187 cm + (3*50 cm) + 25 cm= 362 cm
E	187 cm + (4*50 cm) = 387 cm	187 cm + (4*50 cm) + 25 cm= 412 cm

Table 4.3: Absolute axial sample locations.

For this reason, three samples were located according to method 1 and three additional, but bigger samples located according to method 2, which has an offset of 25 cm compared to method 1.

4.3 Initial graphite inventory

In order to model the production of the radionuclides in the correct way, a starting point is the initial impurity list. This list should include all the impurities present in the virgin graphite, their concentration (e.g. in ppm) and their uncertainty values. Two documents were available at the start of the project. The most recent and reliable is the neutron activation analysis (NAA) performed by SCK·CEN in 2007 (Appendix B). The NAA was performed on some spare blocks of virgin graphite, both for graphite of A and B quality. Realise that these measurements were performed on a single block, while in reality, about 14000 blocks are present in the BR1 core. Therefore this yields only an indication and is not fully representative for all the blocks in the reactor. The reported uncertainties on the element concentrations provide a level of confidence of approximately 65%.
It was possible to perform the activation calculation in an acceptable time, so the complete list was used. This means that no elements were skipped in contrast to the previous work by E. Bravo in 2010[9].Several nuclides like ^{35}Cl, ^{14}N and ^{6}Li are more important, because these are the precursors for ^{36}Cl, ^{14}C and ^{3}H which on their turn have a major influence on the X and Y criteria.

In order to be conservative and with the intension to prefer overestimation instead of an underestimation the uncertainty values were add up to the measured values for each graphite quality. In case the element concentration was below the detection limit, the detection limit was used.
The second available source concerning the impurity concentration was a scanned document from 1954[18], from the manufacturer of the graphite in the United Kingdom. The technique used to measure the impurities at that time was presumed to be ICP-AES (Inductively coupled plasma atomic emission spectroscopy). This document was used as an extension of the 2007 NAA study, because some elements in the last document were missing. Some additional elements like Boron, Lithium, Lead, Bismuth and Beryllium were available in the UK document. This list of impurities is included in Appendix C. In the study of E.Bravo[9], 0.05 ppm (parts per million) of Lithium was used, based on literature values of a study from N. Messaoudi[8]. Having the document of the graphite manufacturer available, the tabulated value of 0.44 ppm for lithium was used in the simulation. The drawback of this document is the distinction between A and B impurity concentration. The only information mentioned is the absorption microscopic cross section, 3.98 barns for graphite A and 4.8 barns for graphite B. The tabulated element concentrations were used for graphite A and B. First there was the intension to increase the impurities of graphite B based on the ratio of the measured microscopic cross sections, but later on, this was rejected. Uncertainties on the measured values are missing. This has been checked with Mr. Verpoucke at SCK·CEN. There was advised to handle an estimated uncertainty of 50%, based on the uncertainties of the individual actions, like e.g. measuring the samples.

Finally, only the concentration for nitrogen was missing, it wasn't listed on both documents. For that reason there has been opted to use the value of 10 ppm for nitrogen in graphite type A and B. This value is based on the average concentration in nuclear graded graphite for nuclear power plants like MAGNOX, AGR and CEA [8]. At present, this is the most trustworthy estimate for nitrogen.
At this moment, all the element concentration are known in ppm. The isotopic distributions [19] in weight percentages have been used to make the rescaling of impurity concentration for each nuclide before implementing it into the computer code. Before the code was able to run, some nuclides needed to be removed because some of them were absent in the cross section library. When no cross section data is available, no calculations could be performed for that nuclide. This occurred for some less important nuclides (e.g. Osmium).

Until now, the graphite material composition in the BR1 MCNP (Monte Carlo N-Particle Transport Code) geometry didn't contained any impurities, except ^{10}B and ^{11}B.
When traditional studies about the power distribution, neutron fluxes and spectra are carried out, these graphite impurities are not required. For previous reactor studies, the boron equivalent was used: 0.38 ppm in graphite A and 1.6 ppm in graphite B.
This amount of boron has the equivalent absorption cross section of all the impurities and therefore has the same effect on the reactivity of the BR1. The advantage of only using the boron impurity in the graphite is the considerable speed up of the computer simulation compared to using the complete impurity list of 232 nuclides. This is ascribed to the time required for searching the reaction cross section for the neutron with a specific energy for a certain nuclide in the large data files.

When adding many impurities, more absorptions of neutrons will occur and the reactivity of the reactor will decrease. The parameter to measure the reactivity of the reactor is the K_{eff} value. The K_{eff} value or neutron multiplication factor is defined in equation 4.1.

$$K_{eff} = \frac{\text{The number of neutrons in the } n^{\text{th}}+1 \text{ generation}}{\text{he number of neutrons in the } n^{\text{th}} \text{ generation}} \tag{4.1}$$

To provide a small example, suppose we start cycle 1 with 5 neutrons. After several scattering reactions, one neutron will escape the geometry, two other neutrons will be absorbed by (n,γ) and (n,p). The last two neutrons will each cause the fission of a U-235 neutron, emitting respectively two and three neutrons. At the end of this cycle, five neutrons are present in the system and therefore the K_{eff} is one. When calculating the K_{eff} with MCNP it will stabilize after a certain time. When performing the computer simulations, 250 generations or cycles is a good value to achieve a stabilized K_{eff} value. When all the impurities were implemented in the complete graphite structure, the K_{eff} decreased below one. This is not realistic because the BR1 has operated with these settings in the past, so a value above one should be correct. The explanation about this sub criticality is straightforward: to many impurities have been added as a result of the combination of both documents and their corresponding uncertainties and detection limits. An acceptable K_{eff} should be slightly above one.

A procedure was proposed during the work to rescale, in this case, reduce the total amount of impurities based on an MCNP criticality simulation. The intention was to relate the simulated K_{eff} value with a known value. Therefore it would be possible to match the simulated reactivity will the real value and use the corresponding impurity concentrations in the model. A confidential BR1 document of 1956 showed that the reactor was critical, a Keff of 1.000 with 434 fuel channels loaded. Running the MCNP simulation with 434 fuel channels loaded resulted in a subcritical core. Hereby, this procedure was not suitable for rescaling the impurity concentrations.

5 Results and discussion

5.1 Introduction

In the work of E. Bravo[9], less information and computer codes were available compared to now, 4 years later. One of the biggest improvements in the current study will be the usage of the Monte Carlo MCNP software. First there is the BR1 3D geometry which was previously reconstructed by E. Malambu based on drawings and the scale model of BR1. Secondly the ability to calculate the neutron flux and spectrum with high accuracy with MCNP. The previous study did not included any reactor geometry, it only used the flux values, measured at certain points in the axial direction of the graphite, through the center of the core. The concentration of some additional impurities is known by a document from the AERE (Atomic Energy Research Establishment) in Harwell, UK, who analysed the nuclear graded graphite before it was shipped to Belgium. Finally, gamma spectrometry results for certain radionuclides from 2011 are available in order to validate the computer calculation.

5.2 Comparison with measurements

Measurements of gamma spectrometry which were carried out in the past (2011) by SCK·CEN will be used as validation for the simulation results.
As shown in the report, 6 radionuclides were measured for sample B and 7 radionuclides for samples D and E. Only the radionuclides which undergo γ – decay are detected, which is relevant. The measured radionuclides were Co-60, Zn-25, Ba-133, Cs-134, Eu-152, Eu-154, Eu-155. The activity and uncertainty is given in Bq/sample (report Appendix A).
These results are represented in Figure 5.1.
In order to see how well the computer simulations are related with the reality, comparison of the simulations with the measurements were carried out. This step is crucial before making justified conclusions based on the results from the simulation

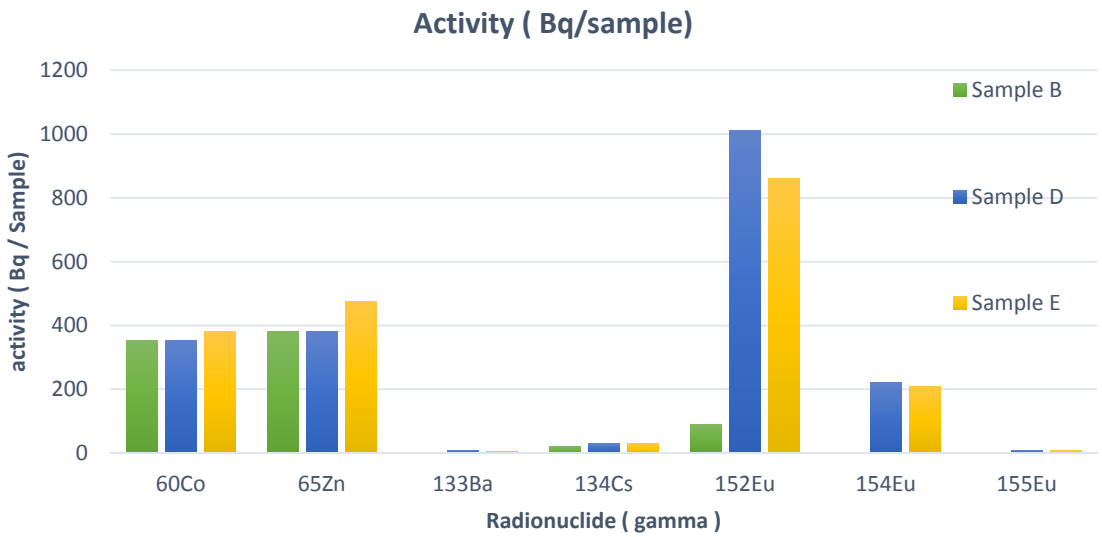

Figure 5.1: Results of gamma spectrometry for irradiated samples B,D and E.

In Figure 5.2 sample B from fuel channel C2.3 is compared with the measurements. Since the exact location of the samples was insure, two possible locations (simulation 1 & 2) for each sample were used, both 25 cm apart from each other. One of both is the correct position. It looks like simulation one matches better with the measurements than the simulation of graphite sample two at position B. For that reason only these (original) positions will be considered.

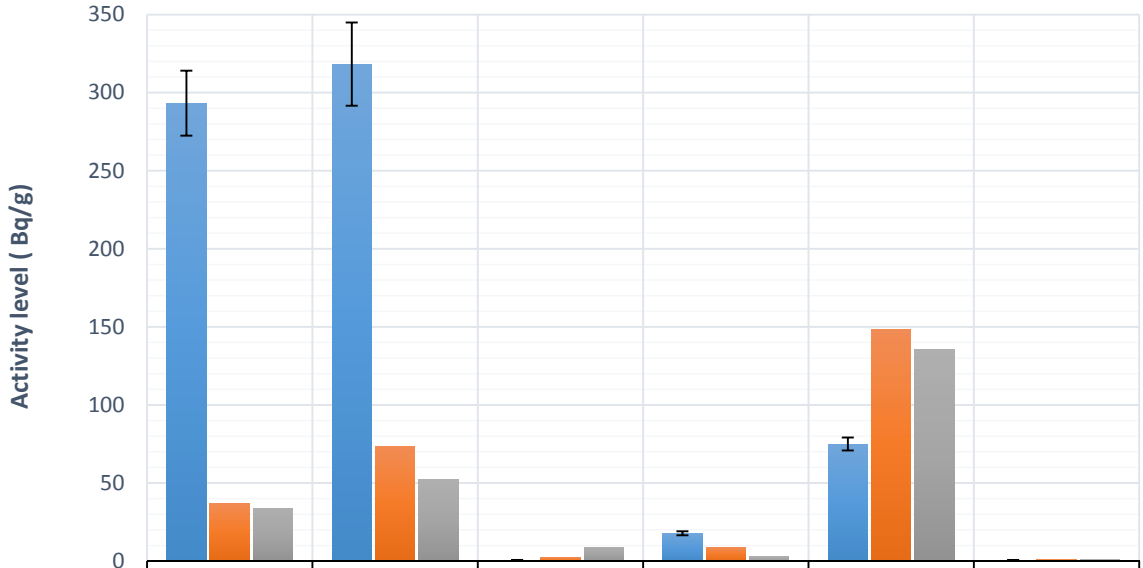

	60Co	65Zn	133Ba	134Cs	152Eu	155Eu
Measurments	293.3	318.3	0.6	17.8	75.0	0.4
Simulation-1	37.14	73.64	2.41	8.48	148.23	0.98
Simulation-2	33.59	52.12	8.87	2.80	135.49	0.94

Figure 5.2: Sample C2.3 B, activity values in Bq/g.

The error bars shown on the measurements are the uncertainties given. For ^{60}Co the simulation result is 37 Bq/g while the measurement was 293 Bq/g. This is a large difference and was not expected because the model of the graphite is quite close the reality. The main reason will probably be the concentration of cobalt in non-irradiated graphite. This is not exactly the same value for each graphite block. For ^{65}Zn, the same observation can be made. An underestimation by a factor 4 to 4.7 was achieved for the specific activity of ^{65}Zn.

The computer simulation results were below the measurements for ^{60}Co, ^{65}Zn and ^{134}Cs, while overestimation occurred for the other radionuclides. There was attempted to find a relationship between the measurement and simulation and the properties of the radionuclide to give a possible scientific explanation. There is no relationship with the half-life. For the lighter nuclei, with A (mass number) 60-65 there appears an underestimation while for the heaver nuclei (A=152-155) an overestimation occurred. These parameters are not related to the computer model in any way and therefore don't give an explanation. What is also a bit strange that ^{152}Eu and ^{155}Eu have different ratios of about 2 and 2.5 overestimation, while they are based on the same impurity concentration of europium. ^{152}Eu is produced by the (n, γ) reaction of ^{151}Eu while in contrast ^{155}Eu is created by beta minus decay of ^{155}Sm. This explains the difference in simulation to measurement ratio. Due to the low concentration of ^{155}Eu is it difficult to explain this difference.

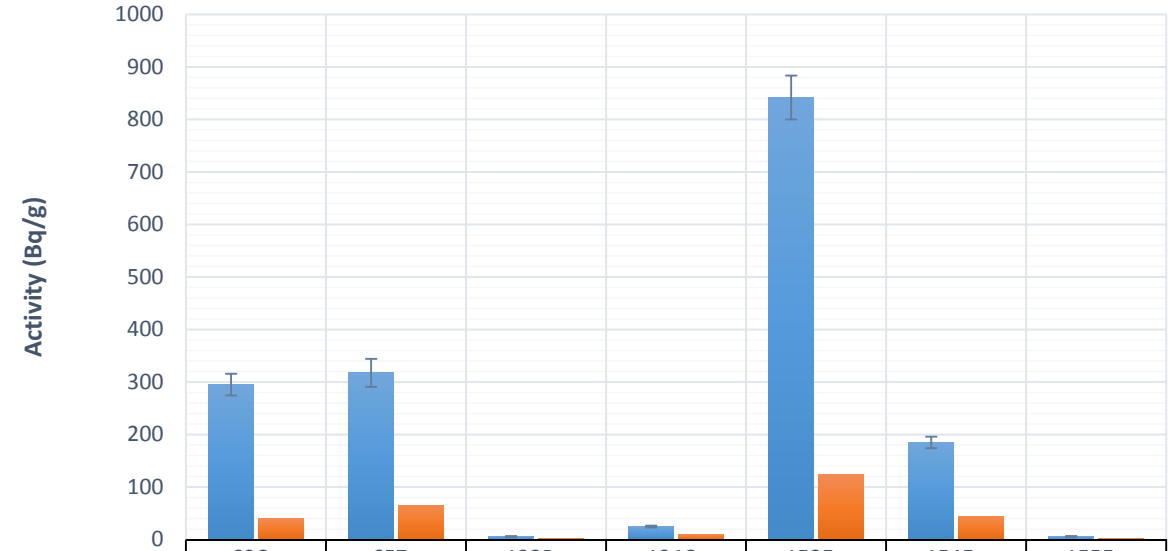

	60Co	65Zn	133Ba	134Cs	152Eu	154Eu	155Eu
Measurements	295.0	317.5	5.8	24.7	841.7	185.0	5.9
Simulation-1	40.18	65.36	2.85	8.76	123.38	44.59	1.17

Figure 5.3: Sample C2.3 D, activity values in Bq/g.

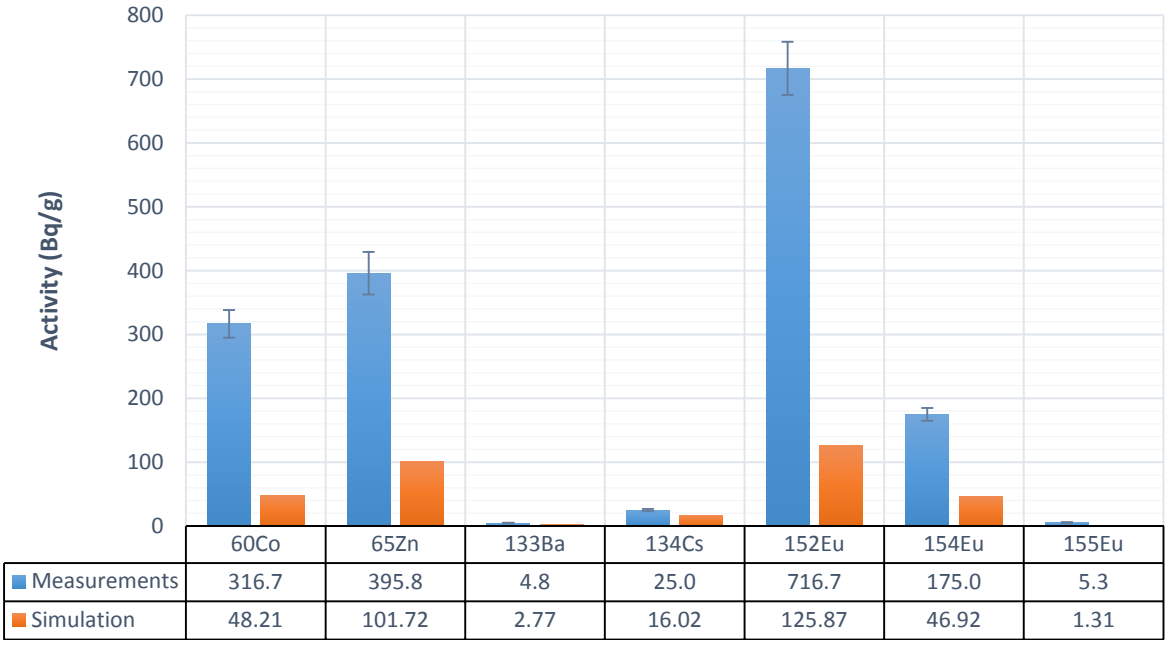

	60Co	65Zn	133Ba	134Cs	152Eu	154Eu	155Eu
Measurements	316.7	395.8	4.8	25.0	716.7	175.0	5.3
Simulation	48.21	101.72	2.77	16.02	125.87	46.92	1.31

Figure 5.4: Sample C2.3 E, activity values in Bq/g.

Based on Figure 5.2 to 5.4, large differences between the measurements and the simulation are observed. For each sample individually, there is no relationship or correction factor that can be used for all the radionuclides. For instance in Figure 5.2, there is an underestimation of a factor 8 on ^{60}Co while at the same time, an overestimation of almost a factor 2 is achieved for ^{152}Eu. This can be attributed to a possible under- and overestimation of the precursors of these radionuclides in the virgin graphite.

For almost all radionuclides for each sample, B, D and E, an underestimation of the computer simulation was observed, except for ^{133}Ba and ^{152}Eu. For sample B, the simulation gave 136 Bq/g compared to the 75 Bq/g of the measurements. For sample D, it is 123 Bq/g compared to 842 Bq/g and for sample D, 126 Bq/g compared to 717 Bq/g for ^{152}Eu (Figures 5.2-5.4).

In addition an inherent uncertainty is present on the computer simulations, which is explained in the next section. Due to the properties of Monte Carlo simulations, even when 2 identical simulation are performed there will be a slightly different result because of the nature of random numbers.

5.3 Comparison with previous simulation study

At the start of the project there was also the intention to compare the simulation results with the results from E. Bravo[9]. Our samples were taken in channel C2.3. Available results from the previous study where only available at different distances in the axial direction, which is the direction of the fuel channels. The activation of radionuclides is strongly position related, therefore is it required that the locations of both simulations (2010 and 2014) for the graphite samples have a certain similarity. A small comparison was done for several radionuclides between sample B, located at minus four cm from the center of the BR1 in axial direction. The best possible value available from the study of E.Bravo was graphite A at the radial distance of 0.5 cm. The results in Bq/g for graphite A quality are illustrated Table 5.1

Radionuclide	ALEPH (Bq/g)	Scenario 2 (Bq/g)	Ratio
H-3	86259.6	3899.8	22.1
C-14	596.3	322.9	1.8
Cl-36	14.9	4.1	3.6
Co-60	37.8	37.5	1.0
Nb-94	85.9	53.5	1.6
Eu-152	150.7	279.9	0.5

Table 5.1: Comparison of activity levels between 2010 and 2014 study.

The activity value of the current simulation was taken at the end of 2010 to compare equal dates with each other. A perfect match is shown between the advanced and simplified computer simulation for ^{60}Co which is remarkable. Larger differences are observed for ^{94}Nb, ^{14}C and ^{36}Cl. The explanation for the very large difference in activity for ^{3}H can be found in the fact that in the current simulation 0.44 ppm of lithium was used, while in the previous simulation only 0.05 ppm was used.

5.4 Uncertainties and simplifications of computer model

The quantification of the magnitude of uncertainty and simplifications in the computer simulation is a difficult task. This is due to the fact that multiple simplifications compared to the reality of the graphite evolution have been carried out. The only manner to quantify the impact of a certain simplification on the final result, in this case the place dependant radionuclide composition and activity is to perform a simulation with different initial parameters. The parameters are for instance the initial impurity composition or the simplified and real geometry of the fuel rod. These additional simulations would consume too much time and therefore will not be performed in the framework of this thesis. This takes too much time and therefore will not be performed. All relevant simplifications and estimated parameters are listed below. Each parameter has an impact on the results.

5.4.1 Impurity concentrations

As shown previously, large differences arise between the production of ^{60}Co and ^{65}Zn in graphite A. The production of these activation products in strongly dependent on the concentration of its precursors, namely cobalt and zinc. These were measured by NAA with listed uncertainties, where the upper concentration was used for the simulation. The upper limits of the measured concentration do not explain why ^{60}Co is up to 7 times and ^{65}Zn 5 times lower than the measurements.

A more solid explanation can be found in the fact that the graphite block on which the impurities where measured in 2007 is a different block then the one the samples were taken in 2011 for radiochemical analysis. Both blocks are of quality A. The first one is a spare block and has never been in the BR1, while the second one has been in the reactor since it was built in 1955. The 3 samples of irradiated graphite have not been taken from the same block but from 2 or 3 separate blocks as how the channel was constructed.

The correlation between the blocks in channel C2.3 as well as the spare block is not known because the measurements of impurities was based on the sample of one block. A variation in impurities between individual blocks is expected and can be quite high but no values can be presented.

A previous study [20] based on experiments showed that all nuclear graphite is different and that no conclusions can be drawn from only one experiment (in our case the NAA measurement of 2007). The study points out that nuclear graphite is a very heterogeneous material with high porosity. Based on their experiences it is advised to use a large set of measurements (around 30 for each radionuclide) to achieved a mean value for each impurity concentration in the graphite. This should be adjusted with a confidence interval depending on the number of measurements.

It would have been good if there was some kind of identification of e.g. based on the batch number of the blocks, which is related to the manufacturing date. This would allow us to identify if the spare block and the blocks in channel C2.3 where from the same batch and therefore have more similar impurity concentrations. On the basis of the construction drawings attempts were made to identify graphite blocks and relate them to the same batch number. Each blocks should be marked and carries a label on the construction drawing. Up until now, unfortunately no relation between the blocks on the drawing and the numbers on the AERA [18] document was discovered.

5.4.2 Modelling of fuel channel C2.3

Channel C2.3 is part of the 80 central channels from which fuel rods were replaced in 1967. Detailed information was available about each fuel rod in the channel over time, which showed that from for instance that from 1967 until 1975 19 fuel rods were present instead of the total of 23. At least 8 fuel zones (instead of the four which were implemented) were required to model the activation of graphite blocks in way it happened in the past.
This was not done because it would increase the simulation time as a result of increasing number of cells and materials for the activation calculation. Also due to the low operating power of the BR1, there were no remarkable differences expected in fuel burn-up between the individual fuel rods.

5.4.3 Irradiation and decay sub step size

As explained in chapter 4,time periods of 1 year have been used for the irradiation history of the BR1. This is not similar to reality where the production and decay occurs continuously. This will have a limited impact on the radioactivity levels . Using smaller time steps, e.g. months or weeks is not possible regarding to calculation times as the evolution calculation time scales almost linear with the number of time steps.

5.4.4 Simplified fuel rod geometry

For the evolution calculation, the fuel rods which consist out of uranium with a silicon cladding and aluminium enclosure where represented as a homogenous mixture of natural uranium, silicon and aluminium with the corresponding mass fractions as the original fuel rod which is an exact representation of the real fuel rod. The impact of the geometry on the graphite activation is not exactly known but is expected to be very low.

5.5 Radionuclide evolution and composition

5.5.1 Radionuclide evolution

As explained in section 4.2.3.3, 44 graphite zones were considered for the evolution calculations. These 44 cylindrical zones were located in 11 channels at the front half of the reactor. Table 5.2 shows the overview of these 11 channels. The light colour represents graphite A, the darker colour graphite B. The official channel number is shown e.g. A0.11 as well as the corresponding universe number (used in the computer model) and also used in Figure 4.13. The radial distances of the volumes ranges from 64.9 cm below the center up the 330 cm in the most outlying position of graphite B in channel A0.18. For convenience material number 200-216 were used to represent graphite B while the numbers 400-426 represent graphite A. These material number don’t have any additional meaning but were used because these are also used by ALEPH in the output file.

Radial distance (cm)	Universe	Channel	Center			Front
			Material numbers			
			0 cm	120 cm	240 cm	300 cm
330	38	A0.18	213	214	215	216
294	37	A0.16	209	210	211	212
258	36	A0.14	424	425	426	208
204	35	A0.11	421	422	423	207
150	34	A0.8	418	419	420	206
114	33	A0.6	415	416	417	205
78	32	A0.4	412	413	414	204
42	31	A0.2	409	410	411	203
6	**30**	**A0.0**	**406**	**407**	**408**	**202**
56.9	29	D1.3	403	404	405	201
64.9	17	C2.3	400	401	402	200

Table 5.2: Locations of 44 graphite zones with corresponding material number

The evolution of the specific activity of some important radionuclides for several graphite locations is shown in this section. This could be done for each of the 20 most dominant radionuclides, however this would lead to too many graphs without additional value to base a conclusion on. There was opted for ^{3}H, ^{14}C, and ^{36}Cl.

Figure 5.5 shows the evolution of ^{3}H production from 1957 up to 2012 in graphite A for different radial positions while the axial positions is located at 0 cm.

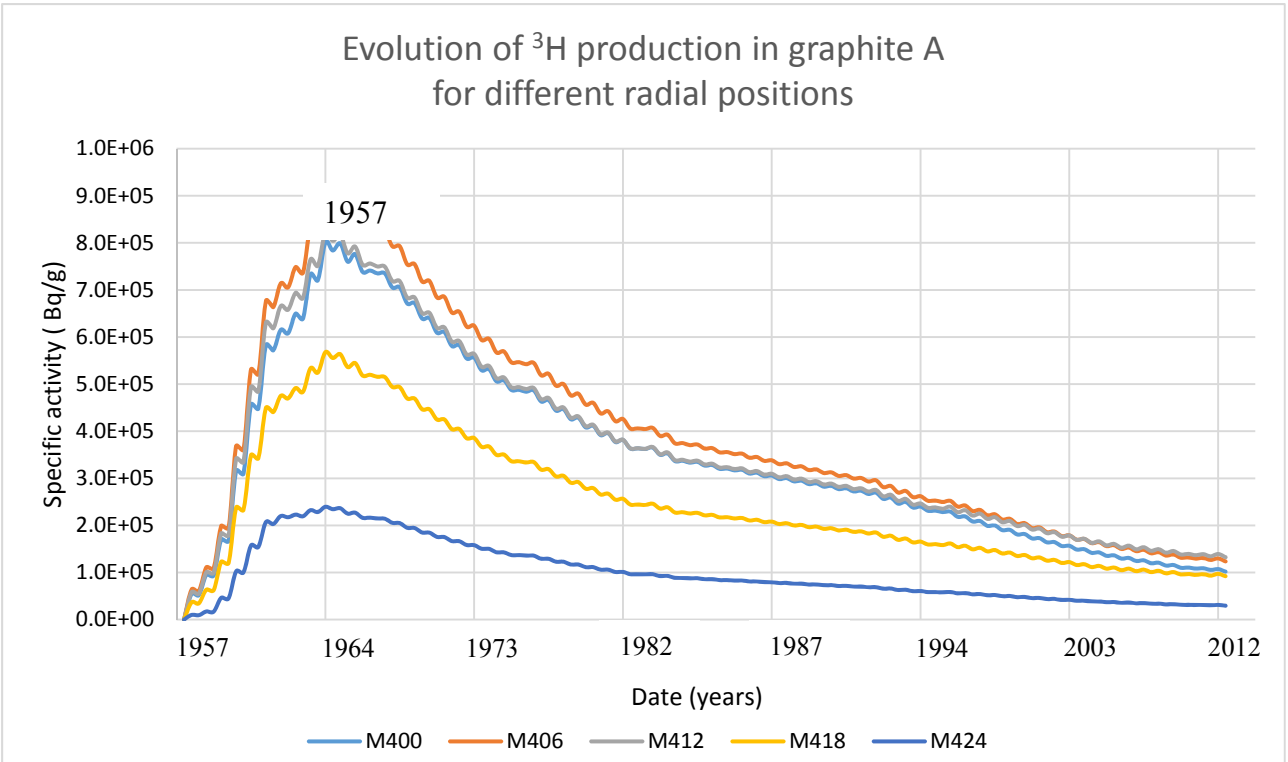

Figure 5.5: Evolution of 3H production in graphite A, axial position at 0 cm.

Due to the relatively short half time of tritium, (12.3 years) only build-up of the activity appeared from the beginning of the BR1 operation until 1964. From 1965 the power reduced significantly as well as ratio irradiation time versus cooling time.
According to the simulation the highest specific activity is reached in material 406, which corresponds to the central channel A0.0. The smallest amount of tritium were produced in material 424, corresponding to channel A0.14. There need to be noted that this was based on an impurity concentration of 0.44 ppm of lithium.

The results for ^{14}C are shown in Figure 5.6 Due to the longer half time, continuous increase of activity is present. The specific activity of ^{14}C is about 3 orders of magnitude lower than ^{3}H.

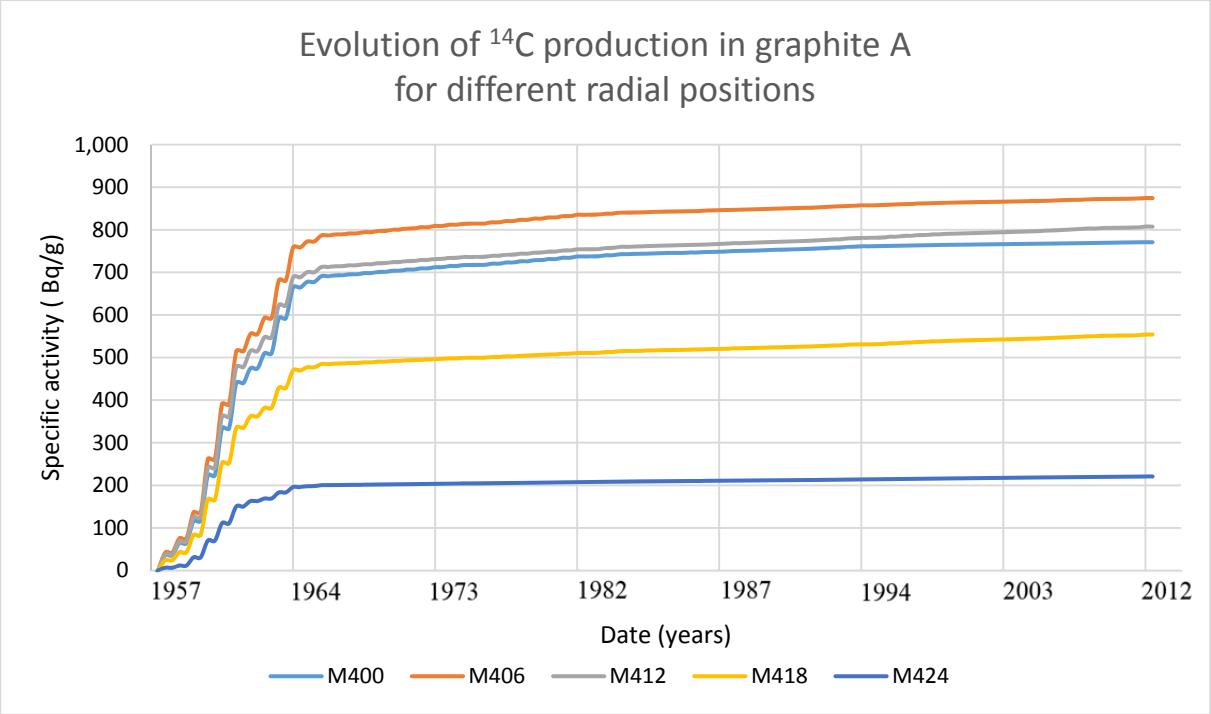

Figure 5.6: Evolution of ^{14}C production in graphite A, axial position at 0 cm.

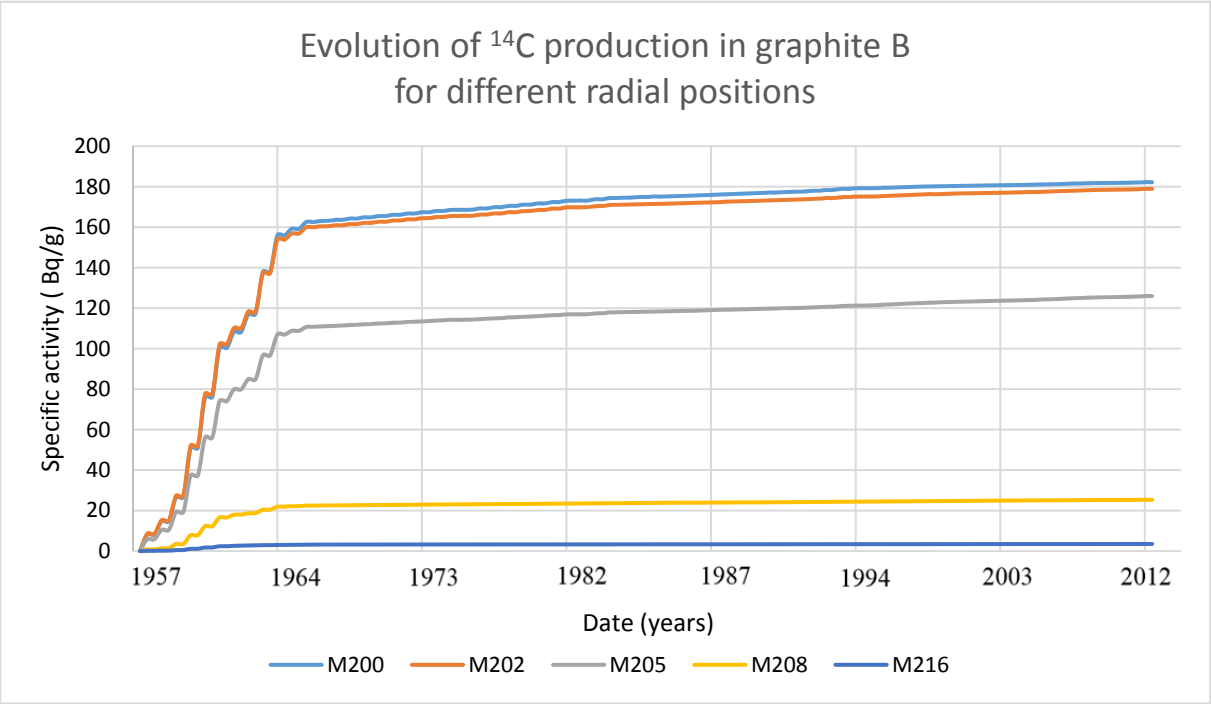

Figure 5.7: Evolution of ^{14}C production in graphite B, axial position at 300 cm.

A similar graph is made for graphite B positions, located at 300 cm (Figure 5.7).
The maximum specific activity for graphite A at the end of 2012 according to the simulation was 874 Bq/g while for graphite B, it was 182 Bq/g. These specific activities are achieved in center of the core. The lowest activity value for Graphite A, material 424 reaches 221 Bq/g while material 216 in graphite B reaches 3.5 Bq/g. Notice the large differences in activity levels between the graphite B locations. Remember that 10 ppm of nitrogen was used, both for graphite A and B.

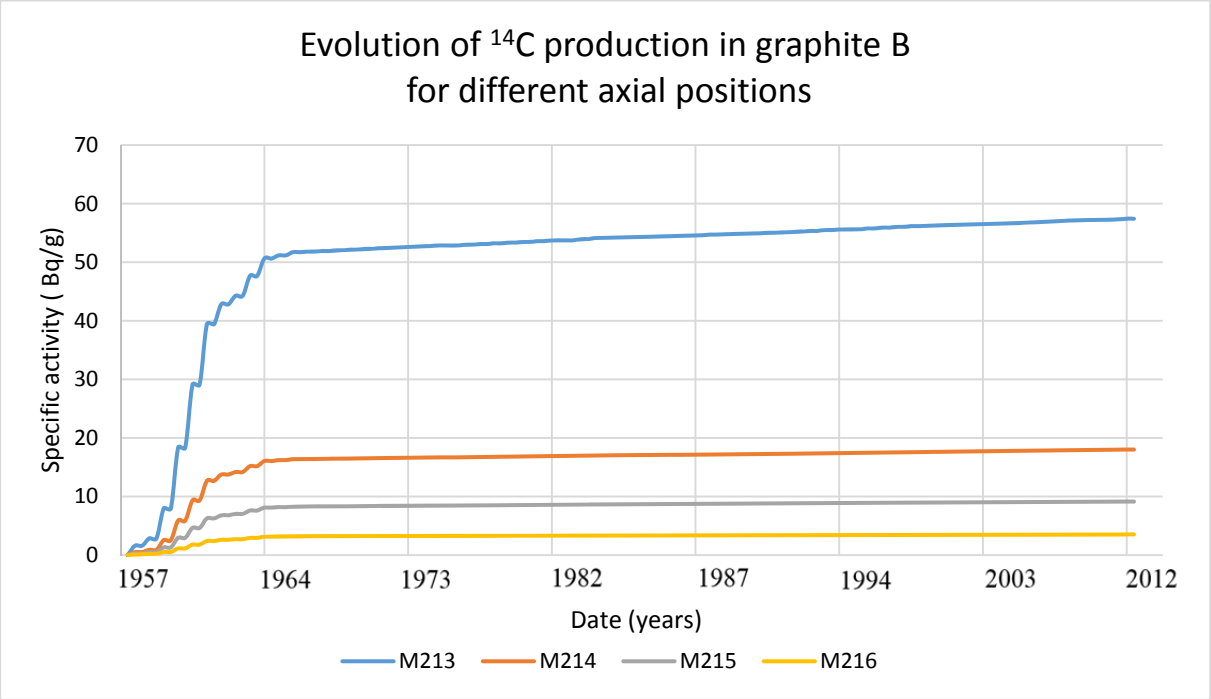

Figure 5.8: Evolution of ^{14}C production in graphite B, axial positions in channel A0.18.

Figure 5.8 represents ^{14}C production in graphite B volumes in channel A0.18. Channel A0.18 is the most outside channel which was used in the evolution calculation, positioned at a radial distance of 330 cm. The activity decreases strongly when the axial distance increases.

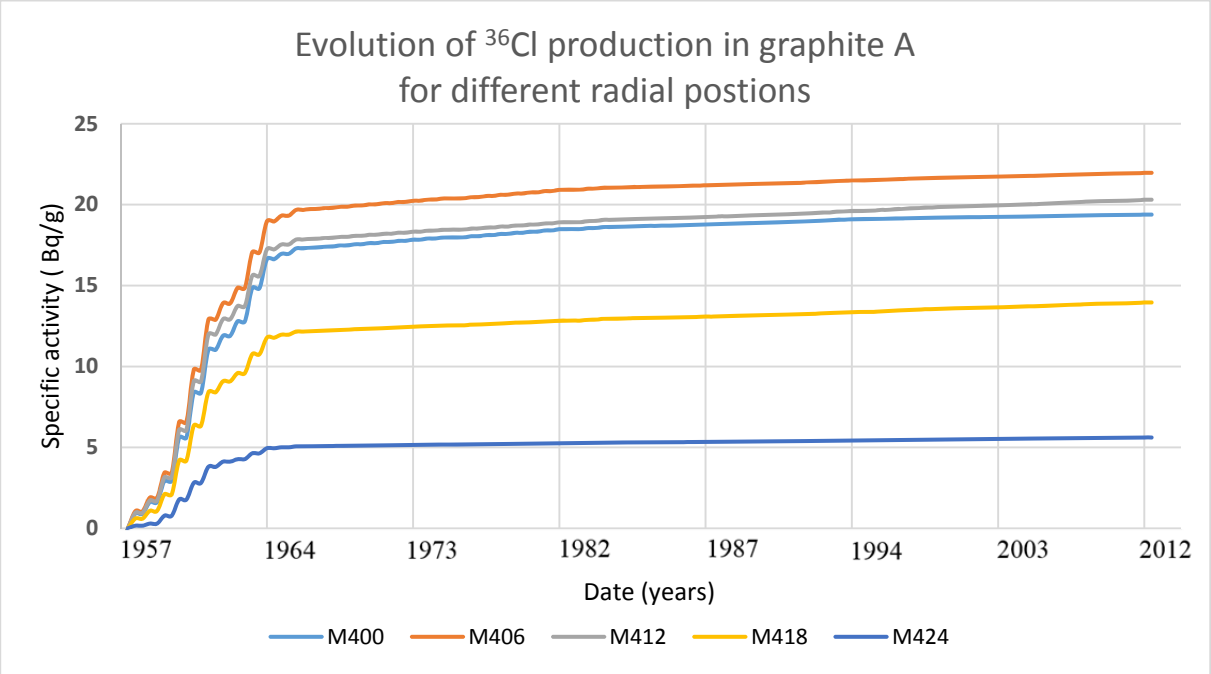

Figure 5.9: Evolution of ^{36}Cl production in graphite A, axial position 0 cm.

Figure 5.9 shows that the ^{36}Cl specific activity ranges between 5.6 and 22 Bq/g for graphite A at the axial position of 0 cm.

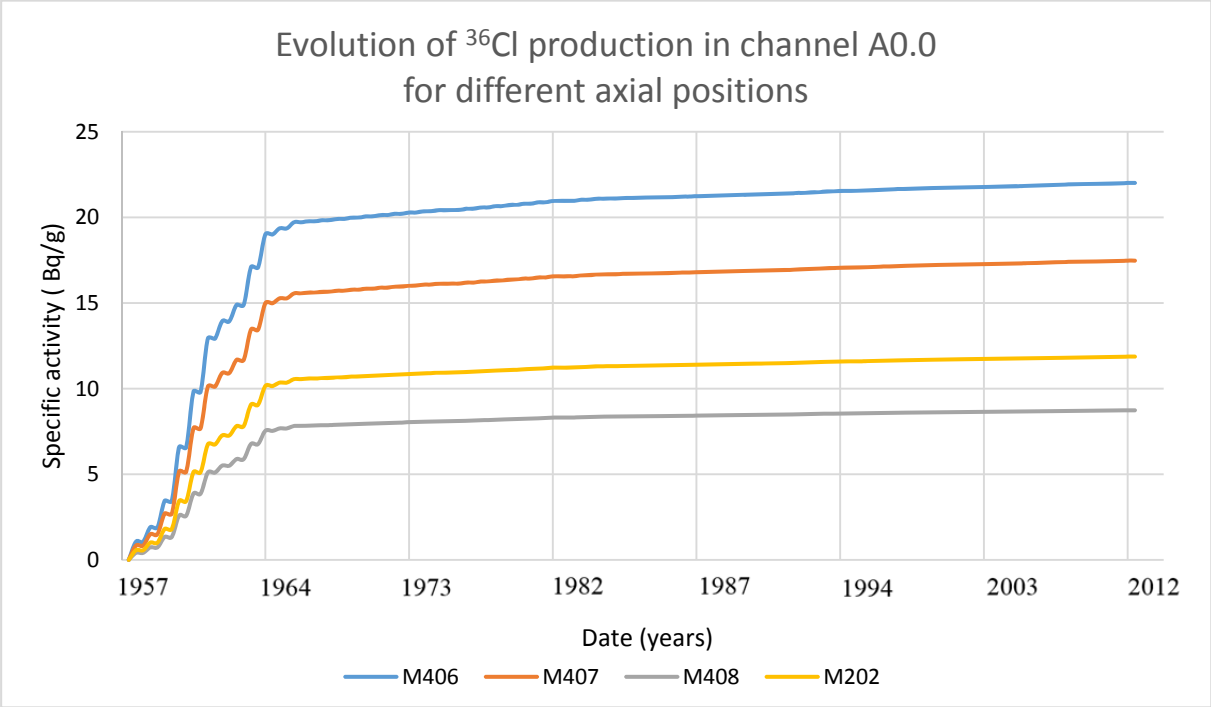

Figure 5.10: Evolution of ^{36}Cl production in channel A0.0, graphite A and B.

Figure 5.10 is very interesting. It confirms what was expected before running the simulation. Material 202, graphite B is located at a distance of 300 cm from the center in channel A0.0 while material 408, graphite A is located at 240 cm and therefore is exposed to a higher neutron flux. Due to the higher chlorine concentrations in graphite B, it exceeds in ^{36}Cl specific activity even if it (graphite B) has lower neutron fluxes at a larger radial distance. Respectively the specific activities are 11.9 Bq/g (graphite B material 202) compared to 8.7 Bq/g (graphite A material 408). The used concentrations for chlorine were 1.92 ppm for graphite A and 5.0 ppm for graphite B.

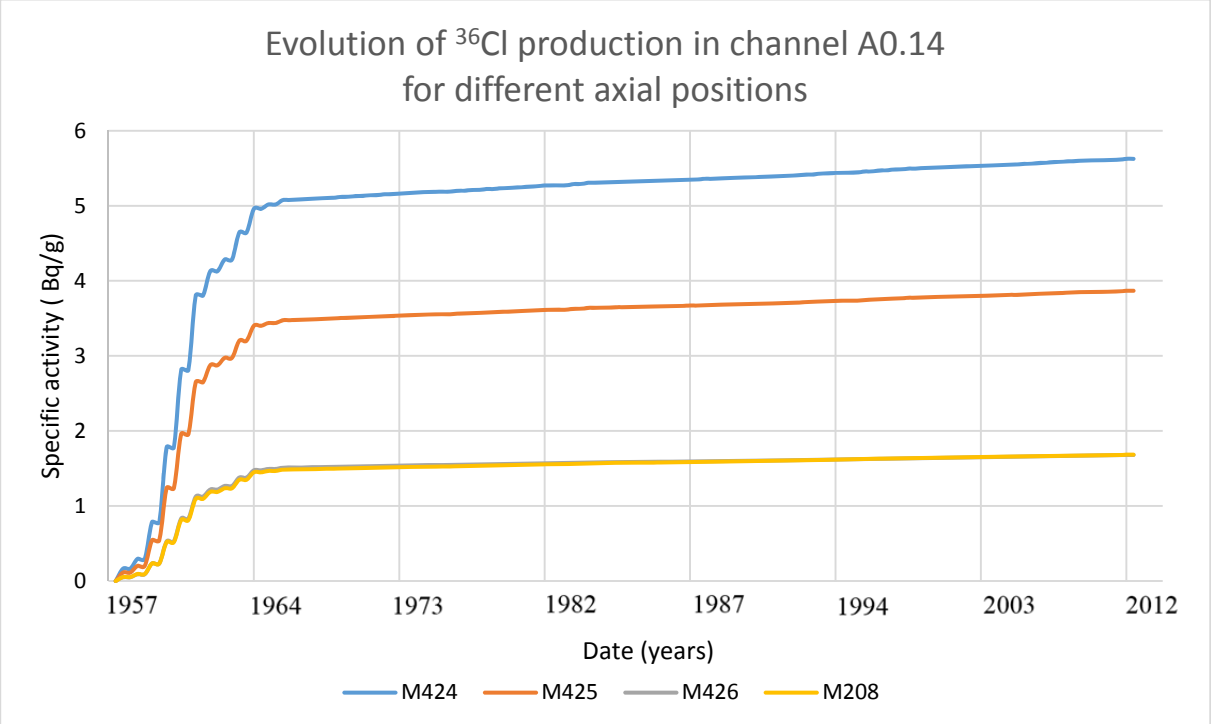

Figure 5.11: Evolution of ^{36}Cl production in l A0.14, graphite A and B.

In figure 5.11 is it shown that ^{36}Cl is produced in almost exact the same quantities in graphite material 426 and 208. The lower neutron flux in graphite B is compensated by the higher concentration of chlorine impurity.

5.5.2 Radionuclide composition

The radionuclide composition of graphite material 216 (graphite B) is shown in figure 5.12 to 5.14. Only the 20 radionuclides which are part of the "critical list" are considered. Other radionuclides are less important regarding the disposal option.

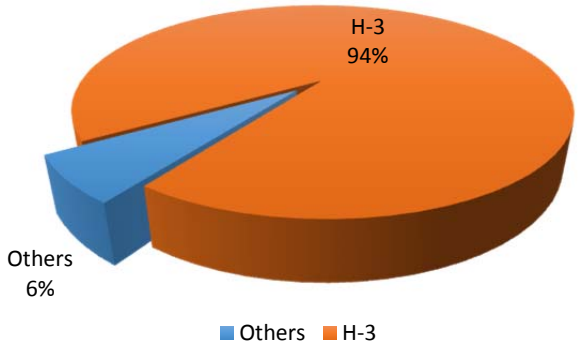

Figure 5.12: Critical radionuclides activity contribution - material 216 - level 1

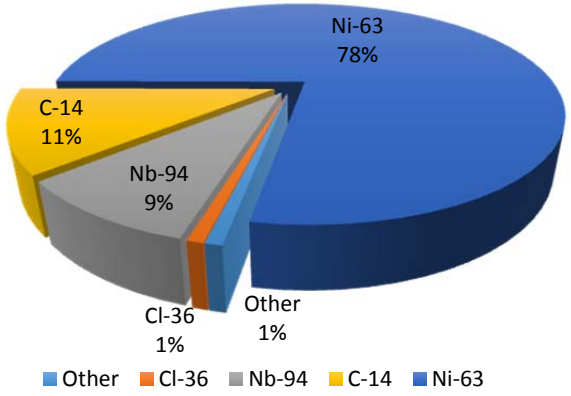

Figure 5.13: Critical radionuclides activity contribution - material 216 - level 2

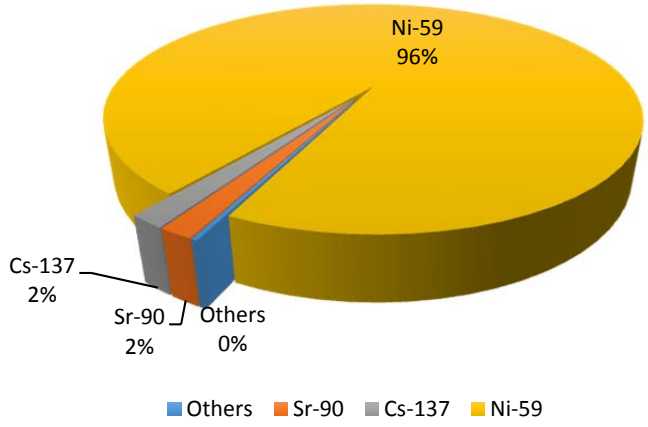

Figure 5.14: Critical radionuclides activity contribution - material 216 - level 3

The previous figures shown that ^{3}H is the most dominant radionuclide in material 216 (graphite B) regarding the activity contribution. This is explained by the fact that ^{6}Li has a large neutron absorption cross section and ^{3}H has a relativity short half-life (12.3 years) compared to ^{63}Ni (100 years), ^{14}C (5730 years) and ^{36}Cl (~300000 years). ^{60}Co is not present in the graphs because it is not one of the 20 critical radionuclides.

5.6 Graphite disposal category

The major goal of this thesis was to determine the disposal option for the graphite.
For each graphite zone, the X and Y criterion values have been calculated to decide the final disposal option for graphite at the end of 2012. It is very interesting to see where the most activated graphite, in terms of the 20 critical radionuclides is located. The graphite volumes at different axial and radial positions, both in graphite A and B were shown in Table 5.2.
Table 5.3 shows the X and Y criterion values for each graphite volume. The X values for the highest activated graphite are far below the value of 1, which means that even with an uncertainty factor of 5, no geological disposal is required.

Material	X - value	Y - value	Material	X - value	Y - value
400	0,128	29,261	**417**	0,034	9,380
401	0,100	23,942	**205**	0,117	13,057
402	0,042	11,990	**418**	0,084	20,902
200	0,175	19,004	**419**	0,066	15,792
403	0,130	31,348	**420**	0,024	7,109
404	0,104	25,246	**206**	0,090	10,144
405	0,043	12,086	**421**	0,052	12,234
201	0,168	18,709	**422**	0,036	9,101
406	0,139	33,033	**423**	0,014	4,128
407	0,109	26,195	**207**	0,052	5,837
408	0,047	12,935	**424**	0,023	8,187
202	0,165	18,525	**425**	0,016	5,639
409	0,130	33,099	**426**	0,007	2,438
410	0,109	26,212	**208**	0,023	2,619
411	0,045	12,486	**209**	0,118	13,313
203	0,156	17,440	**210**	0,079	8,956
412	0,121	30,376	**211**	0,033	3,723
413	0,098	23,601	**212**	0,013	1,459
414	0,041	11,161	**213**	0,052	5,934
204	0,136	15,188	**214**	0,016	1,862
415	0,107	26,338	**215**	0,008	0,945
416	0,082	20,286	**216**	0,003	0,364

Table 5.3: X and Y criterion values for all 44 materials.

The final disposal option for the individual small graphite volumes is represented by Table 5.4. “PSD” stand for possible surface disposal while “SD” stand for surface disposal.

Universe	Channel	Disposal Option			
38	A0.18	PSD	PSD	**SD**	**SD**
37	A0.16	PSD	PSD	PSD	PSD
36	A0.14	PSD	PSD	PSD	PSD
35	A0.11	PSD	PSD	PSD	PSD
34	A0.8	PSD	PSD	PSD	PSD
33	A0.6	PSD	PSD	PSD	PSD
32	A0.4	PSD	PSD	PSD	PSD
31	A0.2	PSD	PSD	PSD	PSD
30	A0.0	PSD	PSD	PSD	PSD
29	D1.3	PSD	PSD	PSD	PSD
17	C2.3	PSD	PSD	PSD	PSD

Table 5.4: Final disposal option based on simulation results.

After applying the acceptance criteria for surface waste disposal, only 2 options (SD and PSD) are acceptable.

Table 5.5 and 5.6 show the detailed results for each of the 20 radionuclides for graphite material 400, graphite A, and material 216, graphite B. This will give better insight in which radionuclide has the highest contribution to the X and Y criterion. There need to be mentioned that the X value should be calculated per waste package, which is standard a 400 l drum. In our case it was done by the volume of the graphite cylinder, which is 70.7 cm^3. When it is calculated for a bigger volume, the activity will be averaged over the volume and slightly lower X values will be achieved.

ALEPH OUTPUT		Ci,max	Ci (Bq/m³) / Ci,max (Bq/m³)	CAi,max	Ci (Bq/m³) / CAi,max (Bq/m³)
Radionuclide	**Bq/m³**	**Bq/m³**		**Bq/m³**	
1-H-3	1,76E+11	1,7E+21	1,033E-10	1,67E+16	1,05E-05
17-Cl-36	3,34E+07	6,0E+13	5,568E-07	1,28E+06	**2,61E+01**
55-Cs-137	1,21E+06	3,9E+11	3,110E-06	1,27E+12	9,55E-07
6-C-14	1,33E+09	6,6E+14	2,013E-06	2,50E+09	5,31E-01
53-I-129	1,93E+01	2,3E+12	8,408E-12	1,62E+05	1,19E-04
41-Nb-94	1,79E+08	1,4E+09	**1,279E-01**	6,83E+07	2,62E+00
28-Ni-59	1,70E+07	1,0E+15	1,702E-08	7,33E+09	2,32E-03
28-Ni-63	1,71E+09	1,6E+15	1,067E-06	1,60E+12	1,067E-03
38-Sr-90	8,55E+05	6,3E+14	1,358E-09	6,67E+10	1,28E-05
43-Tc-99	4,41E+03	1,4E+18	3,153E-15	2,33E+08	1,89E-05
93-Np-237	8,00E-01	1,0E+10	8,004E-11	3,83E+06	2,09E-07
95-Am-241	3,73E+04	4,2E+09	8,884E-06	1,13E+11	3,30E-07
94-Pu-238	2,00E+03	1,5E+10	1,335E-07	6,17E+09	3,25E-07
94-Pu-239	2,02E+05	2,8E+09	7,223E-05	3,83E+07	5,28E-03
94-Pu-240	3,84E+04	2,9E+09	1,326E-05	2,17E+08	1,77E-04
94-Pu-241	1,99E+05	1,2E+11	1,661E-06	3,33E+12	5,99E-08
88-Ra-226	1,82E-03	8,7E+08	2,087E-12	4,83E+07	3,76E-11
92-U-234	2,68E+02	9,0E+09	2,974E-08	4,50E+06	5,95E-05
92-U-235	8,73E+00	5,4E+09	1,617E-09	4,00E+06	2,18E-06
92-U-238	2,22E+02	4,2E+09	5,289E-08	4,17E+06	5,33E-05
SUM		**X criterion**	**0,12803**	**Y criterion**	**29,261**

Table 5.5: Specific activity, X and Y criterion values for graphite A material 400.

The highest specific activity is achieved by tritium. Niobium-94 has the largest impact on the X criterion value while chlorine-36 on the Y criterion value. For graphite A, the measured impurity concentration for ^{94}Nb was below 30 ppm (see Appendix B) which was used for the simulation. This implies that an overestimation has been made. The concentration of chlorine was measured more precisely and the value of 1.92 ppm was used. Due to the high activity of ^{36}Cl, as well as ^{94}Nb, this graphite volume belongs to possible surface disposal. The impact of ^{14}C on the Y value is reasonable, 0.53. In the case for material 216, the X value is largely affected by ^{94}Nb. For the Y value, it is a combination of ^{36}Cl and ^{94}Nb.

ALEPH OUTPUT		Ci,max	Ci (Bq/m³) / Ci,max (Bq/m³)	CAi,max	Ci (Bq/m³) / CAi,max (Bq/m³)
Radionuclide	**Bq/m³**	**Bq/m³**		**Bq/m³**	
1-H-3	7,0845E+08	1,7E+21	4,167E-13	1,67E+16	4,24E-08
17-Cl-36	3,7845E+05	6,0E+13	6,308E-09	1,28E+06	**2,96E-01**
55-Cs-137	6,8034E+03	3,9E+11	1,744E-08	1,27E+12	5,36E-09
6-C-14	5,6969E+06	6,6E+14	8,632E-09	2,50E+09	2,28E-03
53-I-129	1,1935E-01	2,3E+12	5,189E-14	1,62E+05	7,37E-07
41-Nb-94	4,4742E+06	1,4E+09	**3,196E-03**	6,83E+07	6,55E-02
28-Ni-59	3,8334E+05	1,0E+15	3,833E-10	7,33E+09	5,23E-05
28-Ni-63	3,8114E+07	1,6E+15	2,382E-08	1,60E+12	2,382E-05
38-Sr-90	6,3914E+03	6,3E+14	1,015E-11	6,67E+10	9,58E-08
43-Tc-99	1,2777E+01	1,4E+18	9,127E-18	2,33E+08	5,48E-08
93-Np-237	2,3797E-06	1,0E+10	2,380E-16	3,83E+06	6,21E-13
95-Am-241	2,3258E-04	4,2E+09	5,538E-14	1,13E+11	2,06E-15
94-Pu-238	0,0000E+00	1,5E+10	0,000E+00	6,17E+09	0,00E+00
94-Pu-239	2,7179E+02	2,8E+09	9,707E-08	3,83E+07	7,10E-06
94-Pu-240	1,7500E-01	2,9E+09	6,035E-11	2,17E+08	8,06E-10
94-Pu-241	1,4888E-03	1,2E+11	1,241E-14	3,33E+12	4,47E-16
88-Ra-226	2,7742E-03	8,7E+08	3,189E-12	4,83E+07	5,74E-11
92-U-234	4,4781E+02	9,0E+09	4,976E-08	4,50E+06	9,95E-05
92-U-235	2,2103E+01	5,4E+09	4,093E-09	4,00E+06	5,53E-06
92-U-238	4,8040E+02	4,2E+09	1,144E-07	4,17E+06	1,15E-04
SUM		**X criterion**	**0,00320**	**Y criterion**	**0,364**

Table 5.6: Specific activity, X and Y criterion values for graphite B material 216

The least radioactive graphite volume of the 44 simulated volumes, based on the X and Y criterion is located in channel A0.18 at 300 cm in the axial positions in the front part of the pile. It is located inside graphite B blocks and doesn't have any holes.

This graphite is still category A waste, but to confirm, it's radionuclide composition and concentration was compared with the clearance levels for radioactive waste.

The clearance levels and conditions for solid radioactive waste are presented in appendix 1B of the Belgian Royal Decree (20th of July 2001) at the website of FANC/AFCN. The list contains 197 radionuclides. The clearance levels are exceeded for material 216, after checking only 5 radionuclides.

6 Conclusion and outlook

6.1 Computer simulation

Due to the complexity of the calculation, which was not possible without the ALEPH Monte Carlo burn up code, the activation and decay evolution of elements in the BR1 graphite were simulated. A 3D model of the BR1 was already available, but several additional changes were made for optimisation:

(1) Adding the impurity list for graphite type A and B materials. The used impurities were mostly from measurements performed in 2007 by SCK·CEN. The method used was neutron activation analysis. Additional impurity concentration were used from the official document of the graphite manufacturer[18]. The drawback is that no uncertainties were given on these last measurements. Finally, the nitrogen concentration was missing, therefore it was opted to use the literature value[8] of 10 ppm for graphite A as well as graphite B. The Carbowaste EDF study [20] showed that each nuclear graphite is different and therefore the BR1 graphite will be different from graphite used in other reactors.

(2) The fuel loading history has been implemented in ALEPH, a total of six changes took place. Small fuel rod changes will have negligible impact on graphite activation and were ignored due to an increase of calculation time. From 1957 additional fresh fuel was loaded at the outside to compensate the reactivity due to the burn up of the central fuel. In 1967, initial fuel was removed from the core while fresh fuel was inserted, about 1.4 tons in total. In order to make these fuel rod changes more convenient in ALEPH, the fuel rod geometry was changed to a homogeneous element composition. This was combined with the irradiation history of the reactor until the end of 2012 for which information was available.

Several approaches to subdivide the graphite had been considered. The method which has been applied was to regard 11 graphite fuel channels. For each channel, 18 cm in width and height, 4 small cylinders were located: 27 in graphite A en 17 in graphite B. Only these cylindrical volumes contained all the different elements from the large impurity list and were used in the activation calculation. All the graphite outside the small cylinders only contained

the boron equivalent of 0.375 ppm for graphite A en 0.447 ppm for graphite B in addition to the carbon. For that reason, all the graphite, except the volumes where the evolution calculation was performed kept unchanged in material composition. After each core fuel change, the neutron fluxes and spectra were recalculated by MCNP. During a MCNP run, 5.10^5 particles were used for each cycle. 250 cycles were used in total from which the first 50 were inactive cycles. The main reason to choose this parameters was to accomplish the full simulation within several weeks on the SCK·CEN computer cluster.

6.2 Experimental validation

There is no direct correlation between the non-irradiated block where the NAA measurements were performed on in 2007 and the one which has been exposed to neutrons since the 11th of May 1956. It was believed that all of the blocks of graphite A have almost the same impurity concentrations, however, there is no prove of this because only one sample was analysed in 2007.

It's regrettable that no correlation between the blocks was made. This could have been done by placing the graphite of the same batch at different layers in the reactor and to keep for each batch, several spare blocks. This has not been done in 1955 during the construction of the BR1, which is understandable however it would have helped us for this study, almost 60 years later.

The heterogeneity of the graphite blocks can account for large difference in impurity concentrations which had been investigated in a previous study [20]. To have reliable values it was shown that a set of at least 30 measurements is required.

When comparing the available sample measurements of ^{152}Eu by gamma spectrometry, large differences in activity values are observed between the individual irradiated blocks. These results of 75, 842 and 717 Bq/g for the three analysed samples demonstrates a large variation which can not be attributed to the difference in location in the graphite stack.

Final disposal option

6.3 Final disposal option

Based on the current results, which are mostly influenced by the used impurity concentration, in combination with the current methodology of the 20 critical radionuclides and corresponding X and Y criterion published by NIRAS/ONDRAF in 2008, the next conclusion about the disposal option for the 44 graphite zones can be made.
The acceptance criteria for surface disposal show that all the graphite will be considered as possible surface disposal, expect 2 volumes graphite B, located in channel A0.18 at positions of 240 and 300 cm. Possible surface disposal means it has an higher than average activity, but the real action undertaken is not yet decided.

There needs to be concluded that for the majority of the graphite, all graphite A and graphite B with holes can possible be considered for geological disposal. In the most outside massive graphite B blocks, less activation took place, this makes it suited for surface disposal.
The minimum and maximum X criterion value for all the materials are respectively 0.003 and 0.175. This is far below the value of one so effective geological disposal is not the solution.
The dominant radionuclide for this criterion is ^{94}Nb. The reason why exactly this radionuclide is present in high concentrations can be explained by the fact that the detection limits for 30 ppm, respectively 300 ppm were used for niobium in virgin graphite A and B.
Using lower concentration values for niobium should lower the X criterion value, this will not affect the disposal option. For the Y criterion, the values ranges from 0.364 to 33.1. The lowest value is achieved in material 216, graphite B in the most outside location of channel A0.18. In material 409, the highest value was reached which is in the center of channel A0.2.
The dominant radionuclide regarding the disposal option is ^{36}Cl, mainly produced by ^{35}Cl. Lowering this value could result in the transition of graphite sub volumes from possible surface disposal to surface disposal. When the chlorine concentration is halved, this could result in an additional 2 sub volumes for surface disposal. Even when a cooling down period of 50 years was taken into account, it would not change anything due to the long halftime of $3.01 .10^5$ years for ^{36}Cl.

6.4 Future work

When in the next couple of years the work on this subject will be proceeded, there is room for improvement. First of all, a limiting factor during this work was the ignorance regarding the variation in impurities between virgin graphite blocks. This made it also difficult to explain the large variation in activity between the simulation and the measurement for ^{60}Co and ^{65}Zn. Enough virgin graphite blocks are available to perform future measurements on. Secondly, to know the impurity concentrations more precisely, which means to be able to measure elements at lower concentration. (e.g. measuring niobium concentration more precisely). With new presented techniques [21] it is possible to have much lower detection limits. An added value would be to measure the concentration of nitrogen, lithium and boron.

Measuring the activity of ^{36}Cl, which has the major contribution to the Y criterion and therefore decides when geological disposal is required, would be a radionuclide of higher importance to validate the computer simulation with. The radionuclides which were analysed by gamma spectrometry didn't belong to the list of 20 critical radionuclides. The last years, the detection limits of ^{36}Cl have been improved due to new techniques. It is advisable to analyse graphite samples at different axial and radial positions.

It would be good to increase the number of samples taken, for virgin as well as irradiated graphite. In this case, statistical variations would be more easy to observe. Also to take samples both at the left and right position in the reactor. When between those samples, which are taken from the same channel at the same axial distance, large differences are encountered, it could be proved that it is due to inhomogeneity of the blocks.

The acceptance criteria for surface waste disposal are not final yet and need to be approved by FANC/AFCN. This methodology will change in the next couple of years, based on new performance assessments studies carried out by SCK·CEN. This can change the disposal option for activated graphite as well.

Finally, regarding to the computer codes, the evolution calculation of the ALEPH code is currently single-threaded. It means the calculation will only run on a single CPU core, even when 100 cores are available. For the calculation in this work, an irradiation and decay step required about 3 hours of calculation time. When the code is paralysed, all the available cores can be used at the same time. When changes like these are carried out, a large speed-up can be achieved, depending on the number of time steps and materials used in the calculation.

When all these improvements are satisfied, the strategy would be to locate small graphite sub volumes, divided over the complete graphite stack. To perform a first evolution calculation only in these small samples. With the radionuclide inventory and activities, the disposal option can be calculated. At the border between surface and geological disposal, additional sub volumes can be placed and rerun the calculation to contour the difference in waste category more precise. The goal is to minimize the part suited for geological disposal. In the next step, the evolution calculation is to be performed on the complete graphite pile. The division of graphite sub volumes (with the dimension of the real blocks) is based on the previous border. At that time it will maybe be possible to estimate the disposal costs.

Appendix A

SCK·CEN
STUDIECENTRUM VOOR KERNENERGIE
CENTRE D'ETUDE DE L'ENERGIE NUCLEAIRE
Laboratory for Gammaspectrometry
Boeretang 200
B-2400 Mol
tel +32 14 332828
spectro@sckcen.be
http://www.gammaspectrometry.be
Stichting van Openbaar Nut - Fondation d'Utilité publique - Foundation of Public Utility

ISO/IEC 10705:2005 Accredited Laboratory
Authorised Laboratory by FAVV
Member of IAEAs ALMERA Netwerk

BELAC Nr. 015-TEST

10/06/2011

Analysis Report²

Wendy Mertens
SCK SCH
Boeretang 200
2400 Mol

Your order reference:	Order van 2011-05-26	*Our reference:*
Order Description:		2852-5437..5439-XX

Reference Date:	20/05/2011

Sample ID	*Your Sample ID*	*Nuclide*	*Activity*	*Unc*	*Unit*
5437	C2.3.B	^{60}Co	352	25	Bq/ Sample
5437	C2.3.B	^{65}Zn	382	32	Bq/ Sample
5437	C2.3.B	^{133}Ba	0.75	0.12	Bq/ Sample
5437	C2.3.B	^{134}Cs	21.4	1.5	Bq/ Sample
5437	C2.3.B	^{152}Eu	90	5	Bq/ Sample
5437	C2.3.B	^{155}Eu	0.52	0.13	Bq/ Sample
5438	C2.3.D	^{60}Co	354	25	Bq/ Sample
5438	C2.3.D	^{65}Zn	381	32	Bq/ Sample
5438	C2.3.D	^{133}Ba	7.0	0.6	Bq/ Sample
5438	C2.3.D	^{134}Cs	29.6	2.1	Bq/ Sample
5438	C2.3.D	^{152}Eu	1010	50	Bq/ Sample
5438	C2.3.D	^{154}Eu	222	13	Bq/ Sample
5438	C2.3.D	^{155}Eu	7.1	1.1	Bq/ Sample
5439	C2.3.E	^{60}Co	380	26	Bq/ Sample
5439	C2.3.E	^{65}Zn	475	40	Bq/ Sample
5439	C2.3.E	^{133}Ba	5.7	0.5	Bq/ Sample
5439	C2.3.E	^{134}Cs	30.0	2.1	Bq/ Sample
5439	C2.3.E	^{152}Eu	860	50	Bq/ Sample
5439	C2.3.E	^{154}Eu	210	12	Bq/ Sample
5439	C2.3.E	^{155}Eu	6.4	1.0	Bq/ Sample

Analysed By : Leen Verheyen

Approved by : Michel Bruggeman

(1) All reported uncertainties refer to the expanded uncertainty, based upon a standard uncertainty multiplied by a coverage factor of k=2, providing a level of confidence of approximately 95%.

(2) The analysis are based on High Resolution Gamma-ray Spectroscopy using the lab specific method MT.RNM.0001

Page 1 of 1

Appendix B

SCK•CEN
STUDIECENTRUM VOOR KERNENERGIE
CENTRE D'ÉTUDE DE L'ÉNERGIE NUCLÉAIRE

Analysis report

NAA Laboratory – Building GKD
Boeretang 200
B-2400 Mol
Tel.: +32-14-33 27 21 Fax.: +32-14-32 10 56

SCK-CEN – P. Maris
Boeretang 200
B-2400 Mol

Project number:	06-010		
Report number:	06-010	**Date:**	2007-05-23
Sample description:	• Grafiet A • Grafiet B • Van elk van de ontvangen stalen werden drie substalen genomen van ongeveer 1.2 g elk: voor de bepaling van kort, medium en lang levende isotopen		
Sample reception:	2007-04-18		
Irradiation dates:	X727@2007-04-23;X731@2007-05-09;Z728@2007-04-25		
Counting dates:	From 2007-04-25 till 2007-05-20		
Analysis method:	K_0 Neutron Activation Analysis – Panoramic analysis		

Approved by: **P. Vermaercke**
Laboratory Head

BELAC
Nr. 015-TEST

ISO/IEC 17025
Accredited

06-010		GRAFA 72809	GRAFB 72810
F	mg/kg	< 150	< 1.5 %
Na	mg/kg	1.01 ± 0.03	2.49 ± 0.06
Mg	mg/kg	< 15	< 150
Al	mg/kg	< 60 ng/g	4.7 ± 0.5
Si	mg/kg	< 500	< 900
S	mg/kg	< 20	< 300

Cl	mg/kg	1.82 ± 0.1	4.8 ± 0.2
Ar	ng/g	< 3	< 6
K	mg/kg	1.53 ± 0.04	5.6 ± 0.2
Ca	mg/kg	38 ± 3	220 ± 20
Sc	ng/g	19.6 ± 0.5	55 ± 2
Ti	mg/kg	< 4	< 50
V	mg/kg	31.7 ± 0.8	288 ± 7
Cr	mg/kg	0.96 ± 0.07	9.3 ± 0.3
Mn	mg/kg	46 ± 2 ng/g	0.264 ± 0.007
Fe	mg/kg	4.1 ± 0.6	23 ± 2
Co	ng/g	10 ± 2	99 ± 4
Ni	mg/kg	4.5 ± 0.2	23.7 ± 0.6
Cu	mg/kg	0.12 ± 0.03	0.44 ± 0.05
Zn	mg/kg	4.6 ± 0.2	0.48 ± 0.07
Ga	ng/g	< 1	19.4 ± 0.7
Ge	mg/kg	< 0.4	< 0.7
As	ng/g	42 ± 2	58 ± 4
Se	ng/g	< 40	< 90
Br	ng/g	32.4 ± 0.9	57 ± 2
Rb	mg/kg	< 0.2	< 0.3
Sr	mg/kg	0.38 ± 0.02	2.5 ± 0.3
Y	mg/kg	< 1.5	< 4
Zr	mg/kg	< 0.8	< 1.5
Nb	mg/kg	< 30	< 300
Mo	mg/kg	78 ± 7 ng/g	0.24 ± 0.02
Ru	ng/g	< 10	< 40
Rh	mg/kg	< 0.2	< 4
Pd	ng/g	< 5	< 70
Ag	ng/g	< 30	< 50
Cd	ng/g	< 40	< 60
In	ng/g	< 0.3	< 0.5
Sn	mg/kg	< 1.5	< 2
Sb	ng/g	24.4 ± 0.8	6.9 ± 0.4
Te	mg/kg	< 70 ng/g	< 0.15
I	ng/g	< 40	< 80
Cs	ng/g	9 ± 2	18 ± 6
Ba	mg/kg	2.66 ± 0.07	17.7 ± 0.5
La	mg/kg	31.3±0.8 ng/g	0.125 ± 0.003
Ce	mg/kg	73 ± 6 ng/g	0.27 ± 0.02
Pr	ng/g	< 10	38 ± 5
Nd	mg/kg	< 60 ng/g	< 0.3
Sm	ng/g	7.9 ± 0.4	52 ± 2
Eu	ng/g	2.21 ± 0.06	23.8 ± 0.6
Gd	ng/g	< 30	< 70
Tb	ng/g	< 2	< 4
Dy	ng/g	6.4 ± 0.2	20.6 ± 0.6
Ho	ng/g	< 0.6	< 4
Er	ng/g	< 3	< 15
Tm	ng/g	< 5	< 90
Yb	ng/g	22 ± 5	33 ± 2
Lu	ng/g	< 0.5	< 1.5
Hf	ng/g	< 4	22 ± 2
Ta	mg/kg	< 2 ng/g	0.266 ± 0.007
W	ng/g	12.3 ± 0.4	44 ± 2
Re	ng/g	< 0.1	< 1.5
Os	ng/g	< 7	< 20
Ir	ng/g	< 0.3	< 0.7
Pt	mg/kg	< 30 ng/g	< 0.15
Au	ng/g	0.065 ± 0.008	0.08 ± 0.02
Hg	ng/g	39 ± 4	< 70
Th	ng/g	6.4 ± 0.8	44 ± 3
U	ng/g	10 ± 0.5	22 ± 2

Appendix C

Examination of Samples of: Graphite (All figures, except for ash and sulphur content in parts per million)		
Description		**Gleep Test 3.98 mb**
F.B.G. No.		4162
Heat No.		2177/S3
Lab. Serial No.		9155, 9156, 9157, 9158
Date Received		15.12.1953
Source		Harwell
Sample Position		Side Side End End
Ash %		**0.02**
Boron	$_{5}$B	0.15, 0.15, 0.17, 0.13
Iron	$_{26}$Fe	< 10.0
Cadmium	$_{48}$Cd	< 0.03
Lithium	$_{3}$Li	0.44
Sodium	$_{11}$Na	(1.4)
Spectrographic Determinations on ash (Calculated on original material)		
Magnesium	$_{12}$Mg	0.5
Manganese	$_{25}$Mn	0.2
Lead	$_{82}$Pb	0.5
Tin	$_{50}$Sn	0.8
Silicon	$_{14}$Si	40.0
Tungsten	$_{74}$W	< 0.15
Molybdenum	$_{42}$Mo	0.2
Nickel	$_{28}$Ni	3
Bismuth	$_{83}$Bi	< 0.15
Beryllium	$_{4}$Be	< 0.02
Vanadium	$_{23}$V	35
Titanium	$_{22}$Ti	6
Cobalt	$_{27}$Co	< 0.06
Silver	$_{47}$Ag	< 0.1
Zinc	$_{30}$Zn	0.2
Chloride	$_{17}$Cl	4
Sulphor %	**$_{16}$S**	**< 0.01 %**
Chromium	$_{24}$Cr	0.6
Aluminium	$_{13}$Al	2

Calcium	$_{20}$Ca	60
Barium	$_{56}$Ba	3
Strontium	$_{38}$Sr	0.8
Indium	$_{49}$In	< 0.1

Rare Earths, etc.		
Scandium	$_{21}$Sc	0.015
Yttrium	$_{39}$Y	0.035
Lanthanum	$_{57}$La	0.03
Cerium	$_{58}$Ce	0.08
Praseodynium	$_{59}$Pr	< 0.03
Neodymium	$_{60}$Nd	0.04
Samarium	$_{62}$Sm	< 0.025
Europium	$_{63}$Eu	< 0.005
Gadolinium	$_{64}$Gd	< 0.0025
Terbium	$_{65}$Tb	< 0.02
Dysprosium	$_{66}$Dy	< 0.015
Holmium	$_{67}$Ho	< 0.015
Ytterbium	$_{70}$Yb	0.008
Lutecium	$_{71}$Lu	< 0.008

Appendix D

In this thesis the graphite of the BR1, which is in fact the moderator for the neutrons, is studied. A moderator is a crucial material in a nuclear reactor to keep the fission reaction self-sustaining. The fission of a U-235 nucleus is illustrated in Figure 6.1. A neutron collides with a U-235 nucleus which will result in the formation of U-236. The U-236 nucleus will almost immediately break into several parts, 2 fission fragments and several high energetic fissions neutrons. A large amount of variants of fission fragments exists but most likely the fission fragments can be divided in two groups: radionuclides with A (mass number) about 90 and radionuclides with A about 140. The energy distribution of the fission neutrons follow the Watt spectrum, ranging from several KeV (Kilo Electron Volt) up to 20 MeV with the most likely energy of 2 MeV.

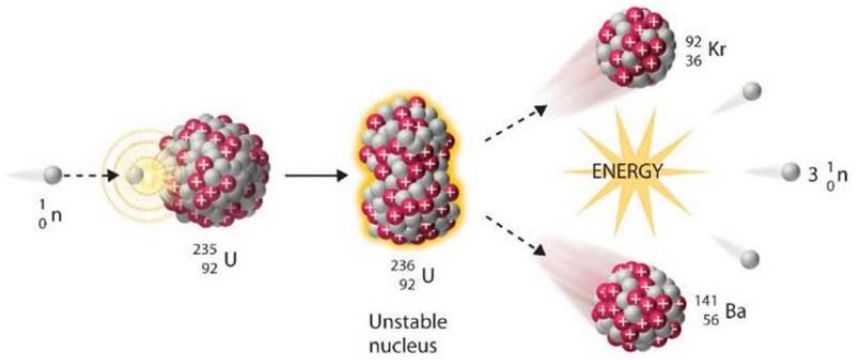

Figure 6.1: Fission of Uranium-235 nucleus.[22]

Consider Figure 6.2 it shows the fission cross section for U-235, which is the probability that a neutron will cause a U-235 nucleus to undergo fission. When considering a neutron energy of 2 MeV, the corresponding cross section equals to about 1 barn. Suppose that the neutron will lose energy to 0.1 eV, which corresponds to a fission cross section of 500 barn. This reduction of neutron energy has increased the fission probability by a factor of 500.

With a cross section of 1 barn, too few fissions would occur, which results in a small amount of fission neutrons. When the fission process with this probability continues, eventually too few neutrons will be present in the reactor to keep the fission chain reaction going on and it will extinguish.

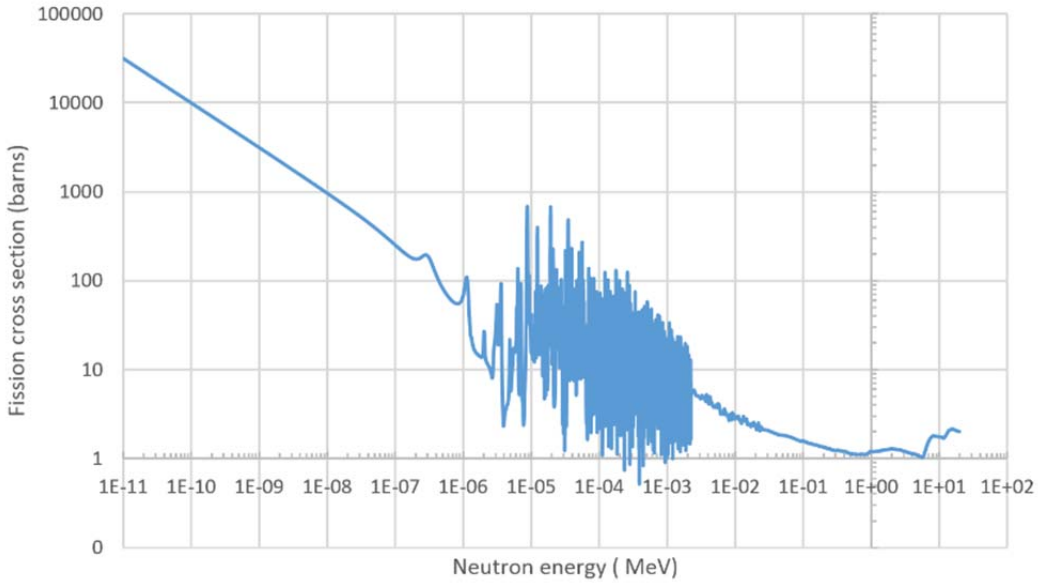

Figure 6.2: Energy dependant fission cross section for Uranium-235. (based on ENDF data)

The reduction of neutron energy is caused by collision between the neutrons and the graphite, more specific the carbon atoms. After each collision a fraction of the neutron energy is transferred to the carbon atom. The neutrons can lose energy in this manner up to a certain point, until it becomes in thermal equilibrium with its environment. In this case the neutrons are labelled full thermal neutrons. Thermal neutrons of 0.0253 eV correspond to a temperature of 20°C. When the BR1 is at a thermal power of 700 kW, the temperature of the graphite is about 100 °C.

Mathematical calculations[23] show that several parameters outline the quality of the moderator. The parameters are the mass number (A), the macroscopic scattering and macroscopic absorption cross section of the moderator atoms. It shows that D_2O is the overall best moderator followed by Carbon (graphite) and H_2O. The reason why H_2O is often used for power reactors is that is it much cheaper than D_2O.

Bibliography

[1] http://www.world-nuclear.org/info/Nuclear-Fuel-Cycle/Power-Reactors/Nuclear-Power-Reactors/

[2] *http://www.world-nuclear.org/info/Nuclear-Fuel-Cycle/Power-Reactors/Appendices/RBMK-Reactors/*

[3] W. VON LENSA et al., "Objectives & Progress of the CARBOWASTE Project - Treatment and Disposal of Irradiated Graphite and other Carbonaceous Waste ", 2011

[4] G. STIENNON et al., "La Pile BR-1 Description, Utilisation et Caracteristiques Physiques", Conférence de Genève, Centre D'etude de L'energie Nucleaire C.E.N., September 1958.

[5] D. Ancius et al., "Evaluation of the activity of irradiated graphite in the Ignalia Nuclear Power Plant RBMK-1500 reactor", Institute of Physics, Vilnius, Lithuania, 2005 NUKLEONIKA 2005;50(3):113-120

[6] E. NARKUNAS et al., "Analysis of Nitrogen Impurity Impact of ^{14}C Generation in RBMK-1500 Reactor Graphite", Lithuanian Energy Institute, Kaunas, Lithuania, 2009 EPRI International Workshop, 6-7 October 2009, Hamburg, Germany

[7] R. PLUKIENE et al. , "Modelling of Impurity Activation in the RBMK Reactor Graphite Using MCNPX", Center for Physical Sciences and Technology, Vilnius, Lithuania, 2011.
Progress in NUCLEAR SCIENCE and TECHNOLOGY, Vol. 2,pp.421-426 (2011)

[8] N. MESSAOUDI. "Caracterization radiologique des matériaux de structure du BR1 – Evaluation de l'activité des matériaux de structure de BR1". Passif technique. SCK·CEN, 2000

[9] E. BRAVO, "Characterization of Irradiated BR1 Graphite", Master thesis BNEN (the Belgian Nuclear higher Education Network), BE (2010)

[10] A. STANKOVSKIY & G. VAN DEN EYNDE,"ALEPH 2.5 A Monte Carlo Burn-up Code User's Manual", SCK·CEN, 2013

[11] P. VAN ISEGHEM,"Radioactive Waste: Conditioning, characterization", BNEN courses on the Nuclear Fuel Cycle, 2013

[12] "Het cAt-project in Dessel – Het Masterplan in vogelvlucht", ONDRAF/NIRAS, *http://www.niras-cat.be/downloads/Brochure%20masterplan%20NL.pdf*

[13] M. DE CRAEN, “Underlying R&D for the selection and characterization of a suitable geological environment for nuclear waste disposal”, SCK·CEN Academy short course, March 2014.

[14] T. GOORLEY, “Criticality Calculations with MCNP5: A Primer”, Los Alamos National Laboratory

[15] SCK·CEN, “50th anniversary BR1”, BR1 history brochure, SCK·CEN, BE (2006), Jan Van der Auwera, Pictures: F. Philippi(1955-1956),B-twee.be

[16] L. LEENDERS, “Etude Physique du Réacteur BR-1 de Mol”, Thesis Physique Nucléaire, BE (octobre 1958)

[17] Veiligheidsrapport BR1, SCK·CEN, 2006

[18] G.H. GREENHALGH, “The Supply of Graphite to Belgium”, Atomic Energy Research Establishment (AERE), Department of atomic energy, Harwell Berks, UK (1954)

[19] L. M. PETRIE, P. B. FOX, K. LUCIUS, “Standard Composition Library”, Oak Ridge National Laboratory, USA (2006)

[20] B. PONCET & L. PETIT, “Operational histories of irradiated graphites – Lessons learnt from the measurements and the radionuclide inventory of i-graphite”, Carbowaste & EDF, Vilnius, 2013

[21] EURADWASTE'13 , 8th EC conference on the Management of Radioactive Waste Community Policy and Research on Disposal (Vilnius, Lituania, 14-16/10/2013)

[22] *http://2012books.lardbucket.org/books/principles-of-general-chemistry-v1.0m/section_24/76a0a494f334a195bab06106babc1e90.jpg*

[23] ELMER E. LEWIS, “Fundamentals of Nuclear Reactor Physics”, Elsevier Inc., USA (2008), p61-63